



Identification of novel indole based heterocycles as selective estrogen receptor modulator

Ramit Singla^a, Kunal Prakash^a, Kunj Bihari Gupta^b, Shishir Upadhyay^c, Monisha Dhiman^b, Vikas Jaitak^{a,*}

^a Department of Pharmaceutical Sciences and Natural Products, Central University of Punjab, Bathinda, India

^b Department of Biochemistry and Microbial Sciences, Central University of Punjab, Bathinda, India

^c Department of Animal Sciences, Central University of Punjab, Bathinda, India

ARTICLE INFO

Article history:

Received 9 March 2018

Revised 4 April 2018

Accepted 6 April 2018

Available online 24 April 2018

Keywords:

Breast cancer

Chromene

Estrogen receptor

Indole derivatives

Dihydropyridine

ABSTRACT

In the present study, we have designed and synthesized indole derivatives by coalescing the indole nucleus with chromene carbonitrile and dihydropyridine nucleus. Two compounds **5c** and **6d** were selected from series **I** and **II** after sequential combinatorial library generation, docking, absorption, distribution, metabolism and excretion (ADME) filtering, anti-proliferative activity, cytotoxicity, and ER- α competitor assay kit by utilizing estrogen receptor- α (ER- α) dominant T47D BC cells line and PBMCS (Peripheral Blood Mononuclear Cells). Cell imaging experiment suggested that both the compounds successfully cross cellular biomembrane and accumulate in nuclear, cytoplasmic and plasma membrane region. Semiquantitative RT-PCR and Western blotting experiments further supported that both compounds reduced the expression of mRNA and receptor protein of ER- α , thereby preventing downstream transactivation and signaling pathway in T47D cells line. Current findings imply that **5c** and **6d** represent novel ER- α antagonists and may be used in the development of chemotherapy for the management of BC.

© 2018 Elsevier Inc. All rights reserved.

1. Introduction

Breast cancer (BC) is the second most widespread cancer and one of the leading causes of mortality among women globally. In clinical practice, a variety of molecular factors are considered for predicting the prognosis and response to therapy of BC patients. Abnormal expression of estrogen receptor (ER) is a salient pathological phenotype in the majority of BC cases. Preeminent levels of estrogens are thought to be associated with the incidence and proliferation of BC. ER- α is a critical growth regulator in BC, and its expression in BC cells is essential for tumor progression [1]. Selective estrogen receptor modulators (SERMs) are the compounds used for thwarting the effect of estrogens in breast tissues. These compounds bind to the ER similar to natural estrogens. However, their effects range from anti-estrogenic in some cases to estrogenic in others depending upon the target site tissues [2–4]. Since the introduction of tamoxifen as first generation SERM, subsequently second and third generation SERMs have been developed with higher efficacy and safety. Currently available SERMs include raloxifene, lasofoxifene, and bazedoxifene which are useful pharmacological agents for the prevention and treatment of

osteoporosis and BC [5,6]. Bazedoxifene is a third generation indole-based SERM, in phase II clinical trial for the treatment of BC [7].

The search for a new and safer SERMs with a simple structure and high efficiency remains desideratum for a better treatment of BC. It is widely accepted that compounds bearing heteroatoms increase the stability of complex by forming hydrogen bonds with the cancer-related protein targets [8]. It has been observed that nitrogen-containing heterocyclic ring imparts a polarized character and helps in establishing an efficient interaction with ER- α [9], and thus have a potential for providing a new paradigm for maintaining the health of women [8,10]. Later, a fusion of two or more heterocyclic rings in a single molecular frame has become an appealing method for drug design. The outcome being a combined pharmacophore having structural features of two or more active substances leading to synergism, enhancement or modulation of the desired characteristics of individual components [11,12]. Another exciting feature of this approach is a generation of a diverse array of pharmacophore which has an extensive application in the field of medicinal chemistry. These molecules can also be modulated for combating the incidence of drug resistance as a single molecule can have different modes of action at the same time thereby reducing the chances of drug resistance [13–15]. In recent years, there has been an arising interest in an indole-fused heterocyclic ring structure in cancer drug discovery [16–19].

* Corresponding author at: Department of Pharmaceutical Sciences and Natural Products, Central University of Punjab, Bathinda, Pb 151001, India.

E-mail address: vikasjaitak@gmail.com (V. Jaitak).

It has been reported that 2-arylindole derivative is selective towards the ER- α and antagonizes the action of estradiol in BC cells and uterus tissues.

Owing to the importance of N-heterocycles in the present study we have designed and synthesized Series I (indole-chromene carbonitrile derivative) and II (indole-dihydropyridine derivative), as putative SERM for targeting ER- α for the management of hormone-dependent BC (HDBC). The synthesized molecules were characterized by NMR and HRMS. Compounds were analyzed for the anticancer activity using ER- α expressing T47D cell lines, ER- α binding assay, semiquantitative RT-PCR, Western blotting and confocal microscopy. Molecular docking was used to identify the possible binding modes of indole derivatives with ER- α .

2. Results and discussion

2.1. Design of indole derivatives

Indole based compounds have a tremendous potential for the development of chemotherapeutic agents [20,21]. Structural analysis of the available literature suggests that 1-benzyl-indole-3-carbinol, an analog of indole-3-carbinol was found to be thousand times more potent in comparison to indole-3-carbinol in the suppression of both estrogen-dependent and independent BC cell lines [22]. Hence, N-benylation significantly improves the anti-proliferative activity as compared to its counterpart. It has been also reported that 2-aryl indole derivative exerts its anti-estrogenic effect by targeting ER- α [19,23]. Similarly, ERA923 is another indole derivative having an anti-estrogenic activity which targets ER- α and is equally effective as tamoxifen and can overcome the resistance associated with tamoxifen [24] (Fig. 1). Bazedoxifene is another indole-based SERM which is known to bind ER- α with a higher affinity as compared to ER- β . In recent years, chromene and acridine derivatives have attracted considerable interest in the development of drug candidates for cancer chemotherapeutics. SAR studies have demonstrated that the aryl substitution at the 4th position of chromenes and acridine compound further potentiates the activity [25]. Among the wide range of biological properties of 1,4-dihydropyridines (DHP) as an anti-cancer moiety, they have also been recognized as multidrug resistance reversing agents in cancer therapy [26,27]. Several reports are published for different derivatives of DHPs including dexniguldipine, niguldipine, nicardipine, and nitrendipine regarding their potent activity in the management of BC by breast cancer receptor protein (BCRP) inhibition [28]. It is well established that slight structural modifications of the DHP ring may result in remarkable changes in pharmacological effects, thereby DHP core has revitalized the interest of the synthetic community. Among different derivatives of 1,4-DHPs, 1,8-acridinedione is a known scaffold with a broad spectrum of biological effects such as DNA intercalating, anti-tumor, and cytotoxic activity [28–31]. Recently, a 1,8-acridinedione derivative (3,3,6,6-Tetramethyl-9-[1-(4-fluorobenzyl)-2-(methylthio)-5-imidazolyl]-2,3,4,5,6,7,9,10-octahydro-1,8-acridinedione) have been reported to be effective at as low as 1 nm in MDR reversal and tamoxifen resistant T47D cell lines [30]. A chromene based derivative, 12-(4-hydroxyphenyl)-9,9-dimethyl-7a,8,9,10,11a,12-hexahydro-11H-benzo[a]xanthen-11-one (6.7 $\mu\text{g}/\text{mL}$) was found to possess more effective anti-proliferative activity than tamoxifen in MCF-7 cells line [32]. In another example, phenyl substituted dioxooctahydroxanthenes derivatives have been found to be active in MCF-7 cell line with an IC_{50} value of 0.02 $\mu\text{mol}/\text{l}$ [33]. Recently, EM-652 which is an active chromene metabolite of EM-800 has been shown to exhibit antiestrogen profile and as in clinical trials for the treatment and prevention of BC. Another chromene derivative, 2-amino-3-cyano-7-dimethyl-

amino-4-(3-methoxy-4,5-methylenedioxyphenyl)-4H-chromene was recognized as a potent apoptosis inducer and has shown the EC_{50} value of 73 nM in T47D cells [25,34]. α -Mangostin isolated from *Garcinia mangostana* has been reported to be effective in BC by the mechanism of arresting the cell cycle, elevating the caspases and aromatase inhibition [35]. α -Mangostin has been found to reduce the expression of ER- α in MCF-7 cell lines [36]. Hence these derivatives could be used as a template for the development of pharmacophore targeting BC. Hence, by rationally combining the structural features of Indole core with chromene and DHP we have designed indole-chromene carbonitrile and indole-dihydropyridine derivatives for targeting BC (Fig. 1).

2.2. Selection of indole derivatives

Molecular simulation techniques supported the selection of compounds for synthesis. Initially, a combinatorial library for the lead structure of Series I and II was generated. The combination of the database of reagents substituting R^1 and R^2 group (Fig. 1) generated 4086 and 4,618,200 compounds for Series I and II respectively.

The generated set of compounds were then evaluated in the two-step procedure. In the first step, ADME was applied for filtering of compounds with the most promising drug-like properties (Table 1) and next step docking to the active site of ER- α for a final selection of compounds with the highest potential activity (Table 2). With the help of qikprop module used during ADME analysis only top-ranked 500 molecules were retained. Calculation of molecular descriptors and ADME analysis minimizes the chances of failure of compounds in early pre-clinical/phase I clinical trials during the drug development process.

The acceptable limits of QP logPo/w (octanol/water partition coefficient) value were taken in the range of -2.0 to 6.5 and with maximum possible oral bioavailability, thus possessing desirable characteristic absorption parameters for a lead drug molecule. Higher than 6.5 value indicates that compounds will tend to have higher lipophilicity and will not be able to solubilize in the aqueous phase for systemic distribution. Log Po/w value lower than -2.5 indicates higher hydrophilicity which in result will hinder the compound from crossing the cellular biomembrane and acting on the target receptor [37]. During absorption, the molecules must cross the epithelial and endothelial cell barriers to reach the target cells. Caco and MDCK prediction assays have been successfully utilized in the study of drug transport. Caco cells have comparable permeability with transport *in vivo* human jejunum, hence establishes a correlation between bioavailability and absorption. But Caco has suffered a disadvantage of variable expression of transporters like P-gp (a P-glycoprotein, a well-recognized efflux transporter in many tissues including brain, kidney, and intestine). Therefore, MDCK (Madin-Darby Canine Kidney) cells are used to study drug efflux and active transport. Numerous studies have demonstrated that human oral drug absorption and permeability coefficient have good correlations. QPP Caco and QPP MDCK have a recommended acceptable value greater than 500 nm/s. Larger the calculated value better the compound permeability through the gut membrane and higher the oral absorption [38]. Thereby, could be absorbed effectively for next phase of blood plasma distribution. Upon absorption, drugs exist in equilibrium binding with plasma albumin for the distribution. The unbound drug is active and reaches the site of action and gets metabolized and/or excreted. QP logK_{hsa} predicts the binding of the compound to human serum albumin and the acceptable limit was taken as -1.5 to 1.5 . Predicted value more than 1.5 signifies higher albumin binding thus lower the fraction of available drug reaching the site of action. On the contrary value less than -1.5 indicates lower binding and hence reduced plasma half-life of the drug. Hence,

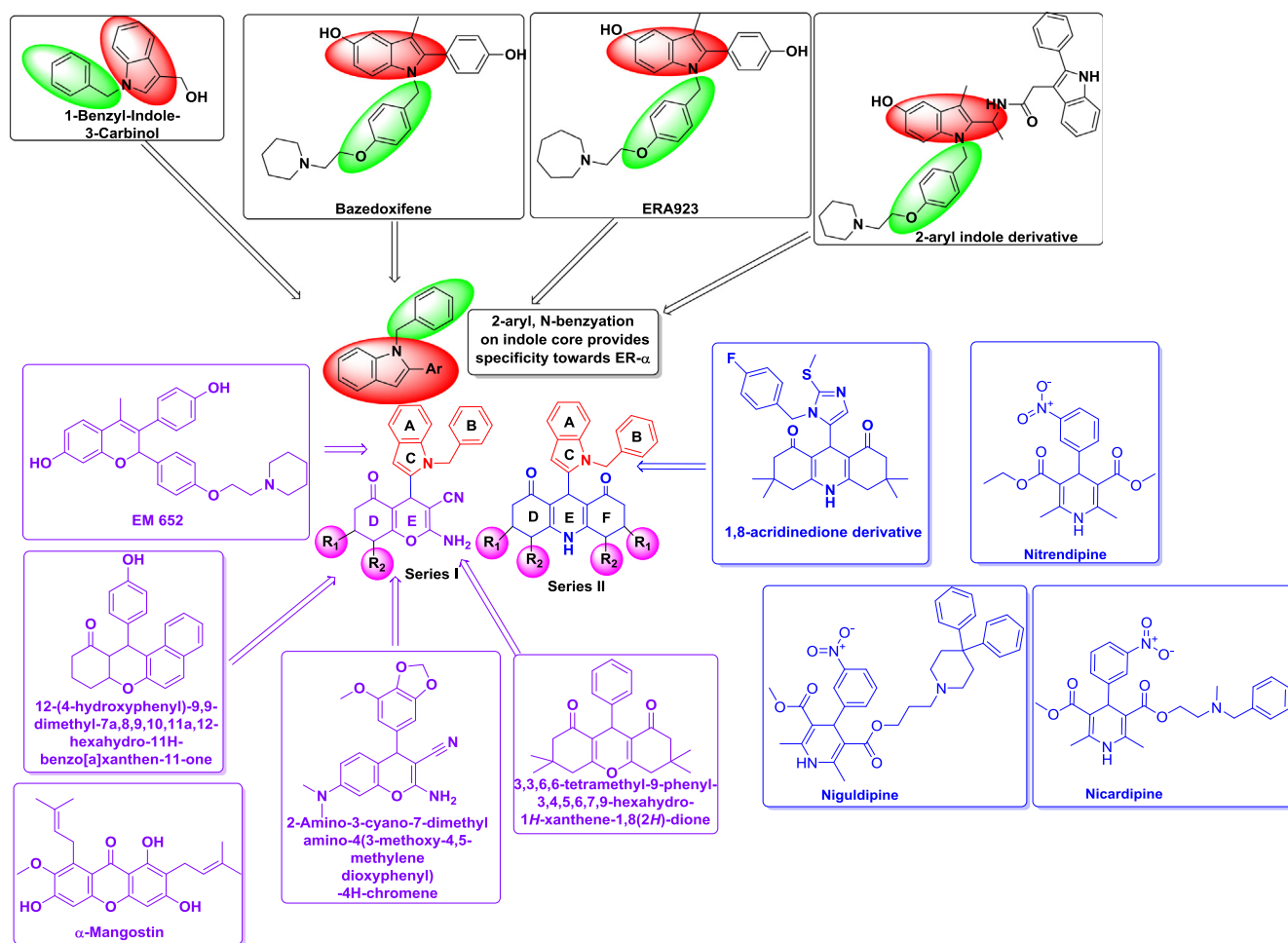


Fig. 1. Designing strategy of indole derivatives.

Table 1
ADME characteristics of indole derivatives selected for synthesis.

Series	S. No	Code	QPlog Po/w	QPlog HERG	QPP Caco (nM/s)	QPP MDCK (nM/s)	QPlogKhsa	Percent human oral absorption
Series I	1	5a	4.90	-5.68	812.92	595.47	1.01	100
	2	5b	4.89	-5.54	793.24	685.14	1.01	100
	3	5c	4.64	-5.79	567.79	868.32	0.94	100
	4	5d	5.95	-7.17	570.05	1069.47	1.40	100
	5	5e	4.25	-5.48	748.69	1261.81	0.74	100
	6	5f	5.50	-6.71	570.04	969.47	1.22	82.56
Series II	7	6a	6.19	-5.18	2502.12	1333.13	1.48	100
	8	6b	6.31	-5.24	2730.50	1465.13	1.63	100
	9	6c	5.94	-6.97	2387.68	1267.35	1.41	100
	10	6d	4.88	-5.80	3612.42	1982.73	1.30	100
	11	6e	4.21	-8.31	2409.08	1279.63	1.49	100
	12	6f	4.16	-8.10	2407.88	7796.06	1.34	100
	13	6g	5.20	-6.93	2370.33	1257.40	1.16	100
	14	6h	4.12	-7.67	2627.63	1405.56	1.06	100
	15	6i	3.98	-7.90	2410.40	1280.39	1.20	100
	16	6j	6.12	-7.57	2474.20	3251.73	1.58	100
	17	6k	6.20	-7.28	2436.51	3198.20	1.33	100
	18	6l	6.44	-7.21	2362.54	3093.37	1.35	100
Standard	Bazedoxifene	-	6.06	-7.45	227.66	110.54	-3.68	91.71

acceptable limit is considered to be optimum in between -1.5 to 1.5. Upon distribution, the drug candidate must be devoid of cardiotoxicity [39]. Several non-cardiovascular drugs have been shown to precipitate cardiotoxicity by blocking the hERG (human ether-a-go-go-related gene) channels which prolongs the QT interval. Thus, in drug discovery and in clinical practice hERG channel is

viewed as primary anti-target [40]. QP log hERG model has been developed for the prediction of IC_{50} value for blockage of this channel. The recommended value is above -5.0, which signifies compounds having a value lower than -5 will tend to activate hERG receptor and may lead to *torsade de pointes* [41]. The ADME analysis identified top 500 compounds which are devoid or have

Table 2
Docking score, H-bond score, Lipophilic EvdW and Electrostatic interaction score of indole derivatives selected for synthesis.

Series	S. No	Code	Docking score (kcal/mol)	XP HBond (kcal/mol)	XP Lipophilic EvdW (kcal/mol)	XP Electro (kcal/mol)
Series I	1	5c	-4.38	-0.70	-6.37	-0.19
	2	5e	-4.31	0	-3.71	-0.15
	3	5b	-3.33	0	-6.17	-0.17
	4	5a	-2.53	-0.60	-6.24	-0.10
	5	5f	-0.95	-0.59	-4.26	0.08
	6	5d	-0.12	0	-2.47	-0.32
Series II	7	6a	-8.05	-0.70	-7.00	-0.25
	8	6b	-7.62	-0.70	-6.88	-0.40
	9	6c	-5.95	-0.41	-5.73	-0.25
	10	6d	-4.41	0	-4.02	-0.09
	11	6g	-3.94	-0.54	-3.93	-0.42
	12	6h	-3.38	-0.35	-3.53	-0.38
	13	6i	-2.95	-0.35	-3.49	-0.41
	14	6e	-2.72	-0.35	-3.22	-0.34
	15	6i	-2.68	-0.51	-3.97	0.07
	16	6k	-2.49	-0.44	-3.27	-0.07
	17	6f	-1.22	0	-3.51	-0.40
	18	6j	-0.07	-0.64	-2.18	-0.39
Standard	Bazedoxifene	-	-9.33	-0.98	-9.53	-0.75

a minimal predicted cardiotoxicity. These 500 molecules were then screened by docking with ER- α for identifying the compounds showing H-bond or Van der Waals interaction with Leu 346. Leu 346 has been reported as an essential amino acid in Helix 12 of ER- α for the antagonistic activity [42]. In addition to the above criteria, cut off docking score was set up as -0.08 kcal/mol. This cutoff score eliminated the compounds which were not showing impressive interaction profile with the target receptor. From the docking filtration criteria, top 50 molecules were selected for further evaluation. Further, 50 molecules were evaluated using the complexity based synthetic accessibility [43]. In this approach, the molecules were evaluated for the availability of synthetic procedures, reagents and building blocks for the synthesis. Collectively on the basis of glide score, favorable ADME profile, and synthesis accessibility six compounds **5a–f** for the lead structure **I** and twelve compounds **6a–l** for lead structure **II** were selected for the synthesis and further evaluation for biological studies.

2.3. Synthesis of indole derivatives

The indole-chromene derivatives (**5a–f**) were synthesized by the general route with high to moderate yields as described in Scheme 1. The N-position of the starting material ethyl indole-2-carboxylate (**1**) was benzylated using benzyl bromide in the presence of potassium hydroxide using DMSO as a polar aprotic solvent to give ethyl-1-benzyl-1H-indole-2-carboxylate (**2**). Compound **2** was reduced to (1-benzyl-1H-indol-2-yl) methanol (**3**) in the presence of LiAlH₄ under dry THF conditions. Compound **3** was oxidized to 1-benzyl-1H-indole-2-carbaldehyde (**4**) by using activated manganese dioxide in dry CH₂Cl₂. A series of indole-chromene derivatives (**5a–f**) were synthesized by one-pot three-component cyclo-condensation reaction of 1-benzyl-1H-indole-2-carbaldehyde (**4**), malononitrile and dimedone. The above mixture upon refluxing in ethanol gives moderate to a good yield, i.e., 69–86%. The plausible mechanism in the literature [44] suggest that the formation of chromene carbonitrile derivative proceeds by in-situ initial formation heterylidenenitrile in the presence of ethanol as a basic catalyst [45]. Heterylidenenitrile formed by the Knoevenagel condensation between 1-benzyl-1H-indole-2-carbaldehyde (**4**) and malononitrile with subsequent loss of water molecules contains electron deficient C=C double bond. In the next step, the Michael addition of dimedone to the unsaturated nitrile which involves the nucleophilic attack of hydroxyl moiety to the

ciano group affords formation of cyclized indole-chromene carbonitrile derivative (Fig. 2).

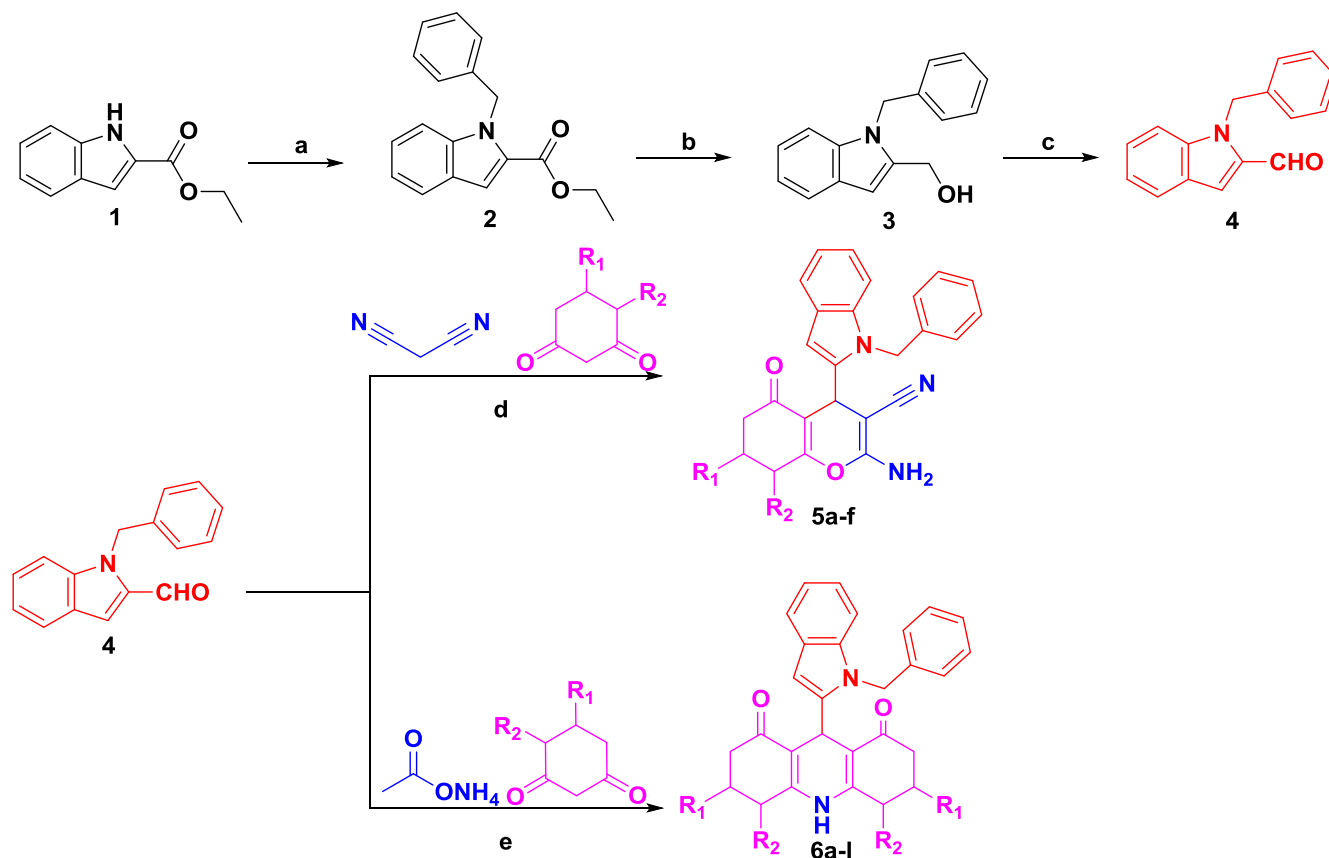
In the compound **5e**, the functional presence of the functional group including amino (NH₂) at C-2, cyanonitrile (CN) at C-3 and carbonyl (C=O) at C-5 was indicated by the appearance of a peak at δ 163.08, 62.20 and 196.12 respectively. The carbon of the cynonitrile group was confirmed by the peak at δ 118.45. The unsaturation between C-4a, 8a was designated by the shift at δ 114.13 and 157.93. Proton for the amino group appears at δ 5.74 and the linkage of the indole with the chromene carbonitrile was confirmed by the δ 27.38 and singlet proton at δ 4.65. HRMS of **5e** showed the peak matching to [M]⁺ for C₂₅H₂₁N₃O₂⁺ at m/z 395.1633. Similarly, other products of the series were confirmed by NMR and HRMS.

The indole-dihydropyridine derivatives (**6a–l**) were prepared by ascorbic acid catalyzed multicomponent Hantzsch dihydropyridine reaction of 1-benzyl-1H-indole-2-carbaldehyde (**4**), dimedone and NH₄OAc in the presence of ethanol at 10 °C. The practical yield was good (65–80%). The reaction proceeds via the enolization of dimedone and 1-benzyl-1H-indole-2-carbaldehyde (**4**) facilitated by ascorbic acid. In the next step intermediated formed by Knoevenagel condensation between aldehyde and dimedone undergoes Michael addition by second molecules of enol form of dimedone (See Fig. 3). The resulting intermediate upon reaction with ammonium acetate yield amine which undergoes intramolecular cyclisation and subsequently dehydration to form indole-dihydropyridine derivative [46].

In compound **6b** the peak at δ 190.10 helped in confirming the carbonyl functional group at C-1 and C-8. The introduction of unsaturation between C-8a,4b and C-9a,4a upon cyclisation was confirmed by the peak at δ 144.88 and 115.41. The characteristic NH proton were observed to give a broad signal at δ 12.16. The bond between indole moiety and dihydropyridine was indicated by the ¹³C signal for C-9 at δ 22.76 and ¹H signal at δ 4.13. HRMS of **6b** showed the peak conforming to [M + 2H]⁺ for C₃₂H₃₆N₂O₂⁺ at m/z 480.2717. Likewise, other congener of the series was spectroscopically identified by ¹H, ¹³C NMR and HRMS. It should be noted that compounds **5a–f** and **6a–l** are novel and were purified using flash chromatography.

2.4. Biological evaluation of indole derivatives

All the synthesized compounds (**5a–f**, **6a–l**) were screened for antiproliferative activity using T47D cell lines which are known



Scheme 1. Reagent and conditions (a) Benzyl bromide, KOH, DMSO, r.t. 1.5 h (b) LiAlH₄, dry THF, 0 °C, 30 min (c) activated MnO₂, dry CH₂Cl₂, r.t., 5 h, (d) malononitrile, dimedone, ethanol, reflux 12–15 h. (e) ammonium acetate, ascorbic acid, dimedone, 10 °C, 9–10 h.

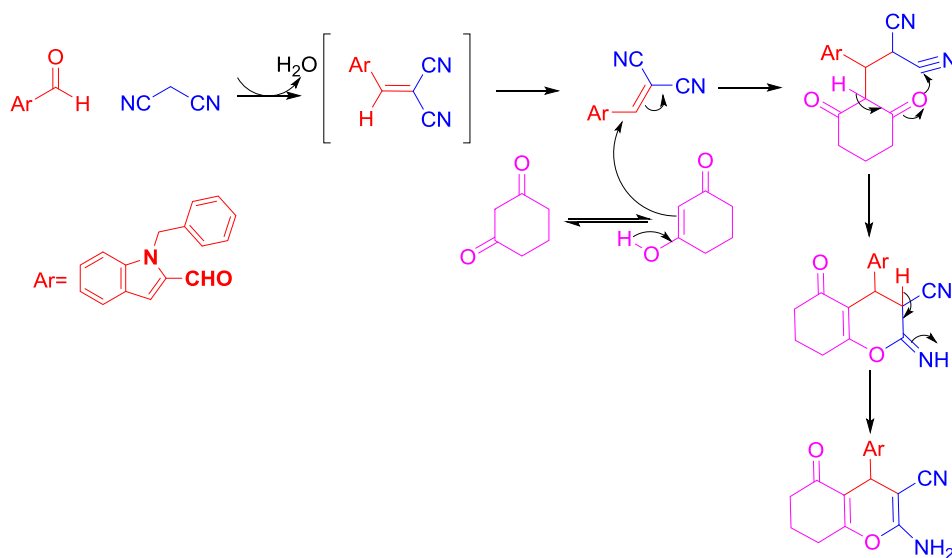


Fig. 2. Plausible mechanistic pathway for the synthesis of indole-chromene carbonitrile derivatives.

for their dominant expression of ER- α (9/1 ratio of ER- α /ER- β expression) [47,48]. All the synthesized compounds (**5a–f**, **6a–l**) were screened for anti-proliferative activity by MTT assay and taking bazedoxifene as positive control using these cells line. Upon analyzing the results of the results from antiproliferative assay, it was found that ten compounds (**5a**, **5b**, **5c**, **6a**, **6b**, **6c**, **6d**, **6g**, **6h** and **6i**) had IC₅₀ in the range of 3.4–24.75 μ M (Table 3). On analyzing

the structural characteristics of the compound, it was observed that alkyl substituent as side chain as in compound **5a**, **5b**, **5c**, **6a**, **6b**, **6c** and **6d** was more active than compounds having classical aryl group as in **5d**, **6e**, **6f**, **6j**, **6k** and **6l**. Such observation indicates that presence of bulky side chains is detrimental and renders the compound inactive at T47D cells line. Majority of chemotherapeutic drugs lacks specificity towards cancerous cells and hence, gets

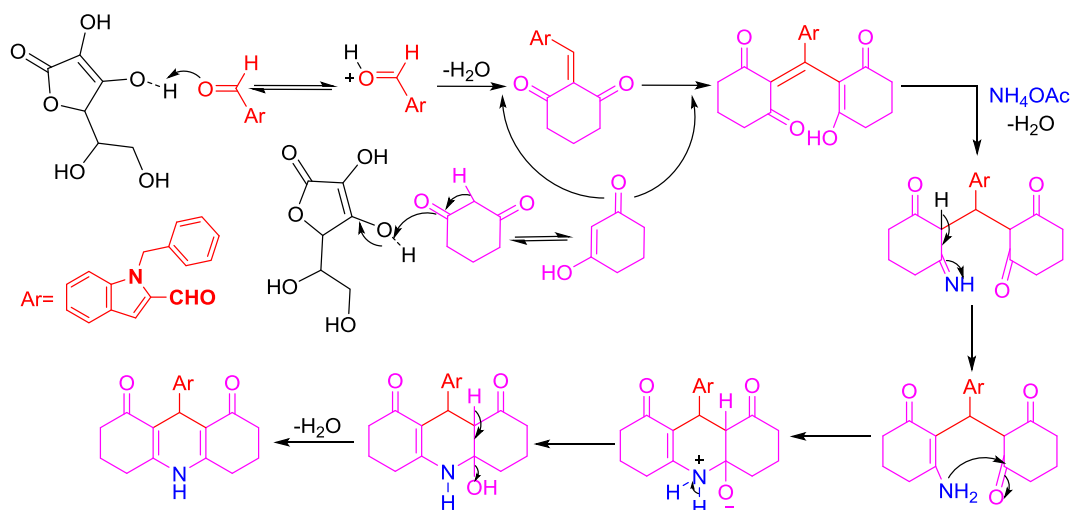


Fig. 3. Plausible mechanistic pathway for the synthesis of indole-dihydropyridine derivatives.

failed in clinical trials. To evaluate the effect of synthesized compounds we further screened the compound of **series I** and **II** for cytotoxicity utilizing human PBMCs (Peripheral Blood Mononuclear Cells) MTT assay. Bazedoxifene (Baz) was also included in the study as a reference standard. PBMC assay indicated that compounds were showing non-significant cytotoxicity even at higher concentration of 100 μM (Fig. 4). Therefore, all the compounds were considerably selective towards the cancerous cells line.

In the expeditious search for the hits targeting BC, the compounds should have binding capacity towards the ER- α . The ER- α binding affinity of all the synthesized compounds was determined by utilizing ER- α competitor assay kit (Polar Screen ER- α Competitor Assay Kit, Green, Life Technology). The principle of the assay is based on the detection of a change in the fluorescence upon competitive displacement of the fluorochrome tagged estrogen by the molecule under investigation from the ER- α -Fluormore™ ES2 complex [49]. This change in the fluorescence is calculated for obtaining the binding affinity of the compound for ER- α . Bazedoxifene was included as the reference standard for comparative study (Table 3). Anti-proliferative bioassay using T47D cells line and binding affinity assay helped in revealing biologically significant structural characteristics present in the synthesized compounds. It was found that compounds having at least one methyl or dimethyl substitution on ring D, F or both were showing best affinity and anti-proliferative activity (Table 3). A similar observation was also observed during the *in silico* screening, the presence of methyl (**5c**, **6c**) or dimethyl (**5a**, **6a**, **5b**, **6b**, **6d**) substituents enables easy ingress of compounds to the receptor site as reflected by higher docking score, higher lipophilic score as compared to other compounds (Table 2, XP lipophilic EvdW). On the other hand, the presence of a classical lipophilic group like phenyl (**5d**, **6e**) and chloro-phenyl (**6f**, **6j**) group were expected to increase the hydrophobic interactions with the receptor. But, on the contrary, these groups renders the compound inactive at both the cellular as well as at the receptor level as indicated by the MTT assay and binding affinity (Table 3). In-depth analysis of the binding confirmation of these compounds revealed that the compounds were not able to bind efficiently at the receptor site of ER- α due to steric hindrance of the bulky side chains (Table 2). Such observations were supported by the lower lipophilic score obtained upon docking of these compound (Table 2, XP lipophilic EvdW). Furthermore, compounds having heterocyclic ring structure such as furan (**6g**, **6i**, **6k**) and benzo[d][1,3]dioxole (**5f**, **6h**, **6l**) as a side chain on D and F ring improved the binding affinity and anti-proliferative activity.

Docking score analysis of these compounds showed that presence of the heterocyclic ring structure adds the factor of hydrogen bonding at the receptor site, thus counteracting the steric hindrance imposed by the bulkiness of the unsaturated ring system. Compounds **5c** and **6d** in series **I** and **II** were escalated for further biological evaluation as this exhibit most potent anti-proliferative activity and binding affinity. Compounds **5c** and **6d** were examined by confocal laser scanning microscopy (CLSM), quantitative RT-PCR and Western blotting for gene expression studies.

With the advancement in technology, there has been a considerable evolution in the development of non-invasive methodologies for determining the distribution of drug molecules in intracellular compartments within intact, living single cells and inside viable cell populations [50]. CLSM is one such technique which eliminates the out of focus light and focuses only narrow regions of the specimen for imaging. An image is built from the fluorescence emitted from the treatment cells and appropriate filtration for background noise. CLSM was used for determining the distribution of the compound **5c** and **6d** inside the T47D cells. The compounds **5c** and **6d** have blue emission, so it was possible to detect the compound using the DAPI excitation-emission channel. The confocal images obtained after the treatment of the compounds **5c** and **6d** after 24 h incubation at 5 and 10 μM respectively indicated that compounds were profusely distributed throughout the nucleoplasm and cytoplasm. Both the compounds were able to cross the cellular bio-membrane, enter the nucleus region of T47D cells. At low biological relevant concentration, compounds were accumulated predominantly in the intracellular region and partially in the intranuclear region. Thus, the confocal images undoubtedly indicate that the compounds were able to interact with proteins present in the nucleoplasm, cytoplasm and plasma membrane (Fig. 5). Thereby, such protein interactions support our concept of anti-cancer activity of these compounds.

It is reported that there is elevated levels of mRNA for ER- α in BC progression is one of the important factor [51]. A decrease in the mRNA level can be expected if synthesized molecules are active and have a high affinity for ER- α . Since, the compounds **5c** and **6d** have shown effective anti-proliferative activity, strong binding affinity and were able to enter and profusely distribute in the cytoplasm, nucleoplasm and cell membrane of the T47D cells line hence were further evaluated for assessing their effect of on the abundance of mRNA of ER- α in human T47D cells line. The mRNA level of ER- α was determined by semi-quantitative RT-PCR using specific primers chosen from human DNA sequences and amplified

Table 3
Structure and biological evaluation of the synthesized indole derivatives.

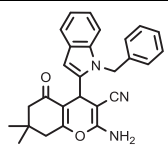
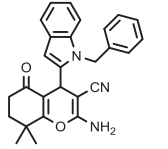
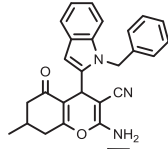
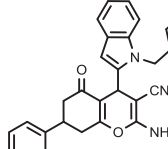
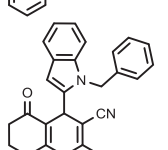
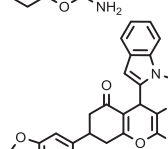
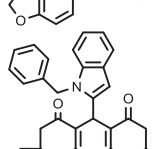
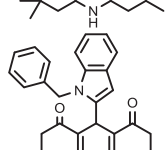
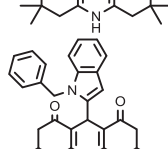
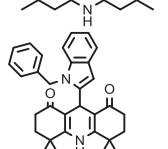
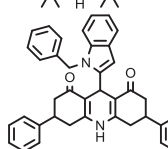
S. No	Code	Anti-proliferative activity using T47D cell line, IC ₅₀ = μM	Binding affinity with ER-α, IC ₅₀ = nM	Structure
1	5a	4.8 ± 0.71	153.04 ± 4.39	
2	5b	3.4 ± 0.67	65.96 ± 0.91	
3	5c	3.8 ± 0.54	64.8 ± 0.11	
4	5d	ND	ND	
5	5e	ND	ND	
6	5f	ND	60.78 ± 0.11	
7	6a	18.22 ± 0.88	74.12 ± 0.29	
8	6b	15.76 ± 1.78	73.15 ± 1.56	
9	6c	24.75 ± 0.04	94.72 ± 2.63	
10	6d	14.63 ± 1.07	52.74 ± 1.33	
11	6e	ND	ND	

Table 3 (continued)

S. No	Code	Anti-proliferative activity using T47D cell line, IC ₅₀ = μM	Binding affinity with ER-α, IC ₅₀ = nM	Structure
12	6f	ND	ND	
13	6g	23 ± 0.02	65.91 ± 0.06	
14	6h	23.98 ± 0.48	67.58 ± 7.73	
15	6i	22.72 ± 0.56	90.46 ± 4.03	
16	6j	ND	ND	
17	6k	ND	96.27 ± 9.12	
18	6l	ND	87.92 ± 6.16	
19	Baz	16.43 ± 0.94	31.71 ± 1.41	

ND: Not determined as IC₅₀ > 25 μM on T47D cell line and binding affinity IC₅₀ > 1000 nM.

in simpliAmp thermal cycler (Applied biosystem). Upon analyzing the agarose gel image and densitometric analysis (Fig. 6), it can be confirmed that the expression of the mRNA of ER-α is completely inhibited in the T47D cells treated with bazedoxifene, **5c**, and **6d** as compared to the control (untreated) cells. Thus, it can be concluded that compounds **5c** and **6d** decreases the expression of ER-α at the transcription level effectively similar to the standard bazedoxifene, thereby downregulating the signaling and transactivation pathways.

Western blot has been widely for understanding the effect of the investigational drugs on the target protein levels. Herein we also utilized for quantifying the effect of lead molecules on the expression of ER-α. Frequently, elevated levels of ER-α are associated with the propagation and survival of BC cells. Non-genomic and genomic pathways rely on the activation mediated by co-activators affiliated with ER-α [52]. Hence, it could be anticipated that reduction in the inherent levels of ER-α leads to superior management of BC.

In our earlier experimental results from semi-quantitative RT-PCR confirm the potent activity of the compounds at mRNA level. Therefore, for extending and confirming the results of RT-PCR, Western blotting was performed. Subsequent analysis obtained from the Western blot image and the densitometry analysis revealed that expression of the ER-α protein was reduced to 20.94% and 28.17% in the T47D cells treated with compound **5c** and **6d** respectively (Fig. 7). While comparing the mRNA level and the protein level of ER-α, it was observed that both the compounds completely inhibited the mRNA of ER-α but slightly reduced protein levels of ER-α. The results suggest that receptor degradation by the compounds was without the contribution of the neosynthesized ER-α pool (pre-formed ER-α). The compounds may be effective only in the newly synthesized ER-α, as the receptor undergoes post-translational modification which can result in reduced drug-receptor interaction. Similar results were obtained with naringenin on the mRNA and protein levels of ER-α [53]. It signifies that compound **5c** and **6d** not only downregulate the

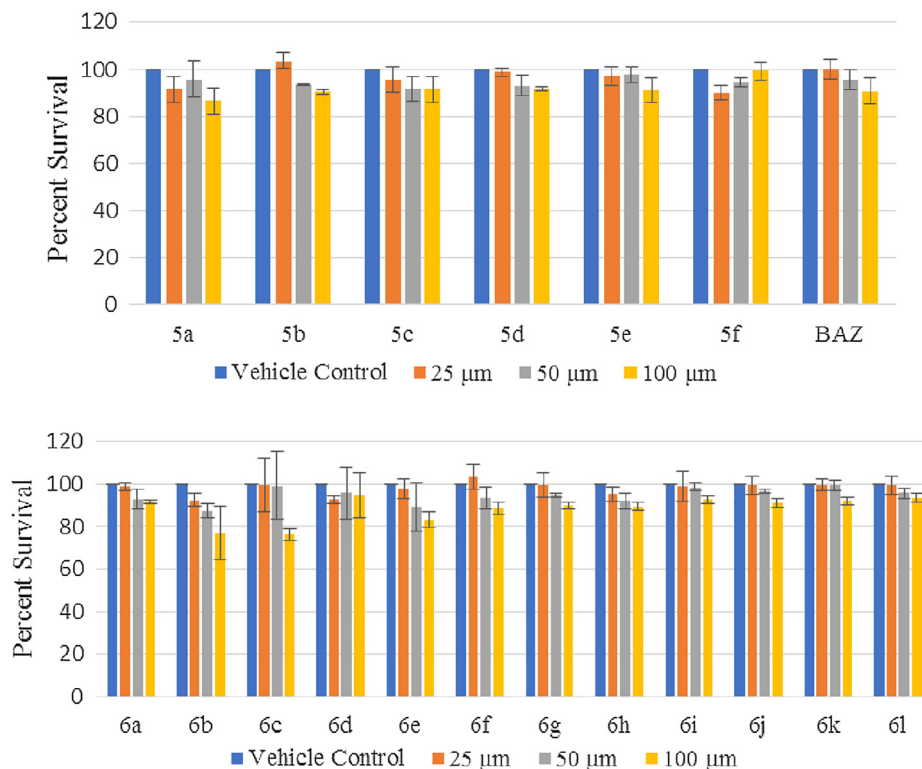


Fig. 4. Human peripheral blood mononuclear cells assay for compound of Series I and II.

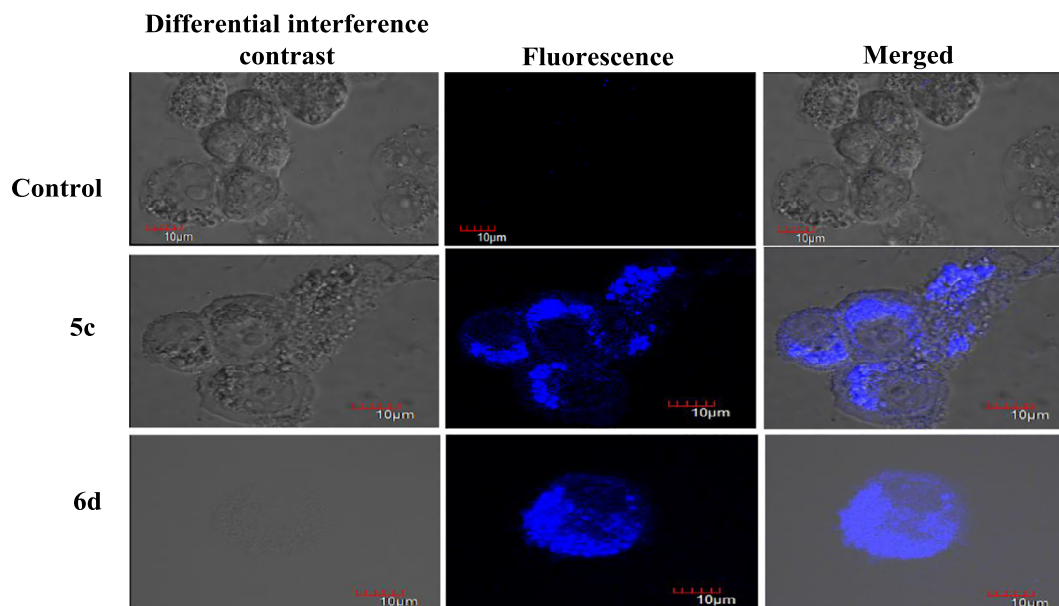


Fig. 5. CLSM analysis of T47D cells after treating the cells with compound 5c and 6d for 24 h and untreated cells as a control (Scale bar, 10 μM).

mRNA of the ER- α but also reduces its protein levels in BC cells. Therefore, synthesized compounds **5c** and **6d** exerts its anticancer activity in T47D cells by targeting the expression of mRNA and protein of ER- α .

2.5. Structural investigation of lead compounds by induced fit docking

The lead compounds and bazedoxifene were analyzed for the mechanistic insight with receptor using induced fit docking approach. The validation of the docking protocol was done by

redocking the co-crystallized bazedoxifene present in the receptor and RMSD was calculated which was found to be 0.02 Å. The similar occupancy as reflected by RMSD and superposition diagram (Fig. 8) signifies that bazedoxifene upon docking recapitulates the confirmation resembling its natural antagonistic confirmation with the ER- α .

The superposition diagram revealed that the lead compounds and bazedoxifene bind in similar confirmation and binding cavity of the receptor (Fig. 9a, c). The compounds were able to form H-bond interaction with Glu 353, Arg 394 and π - π stacking with

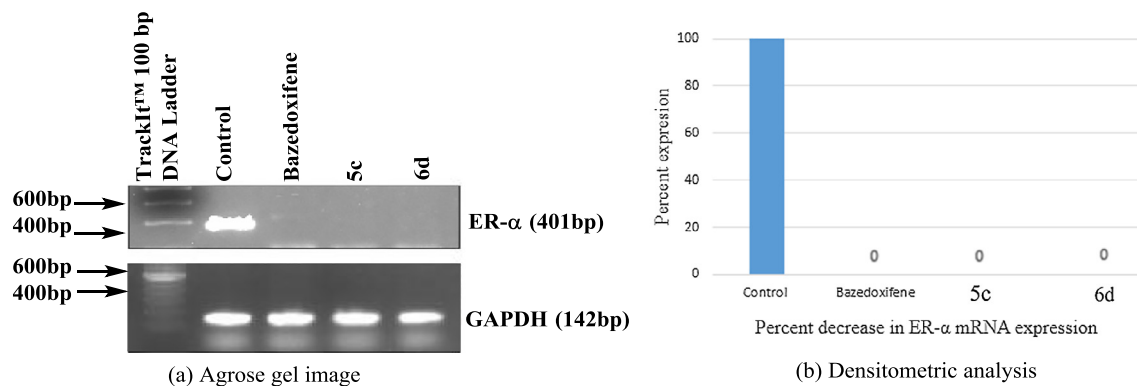


Fig. 6. mRNA expression profile of endogenous ER- α in the T47D cell line after treatment with bazedoxifene and synthesized compounds 5c and 6d. The cells were incubated with 15, 5 and 10 μ M bazedoxifene, 5c and 6d for 48 h respectively. Data were normalized with GAPDH as an internal control, the results shown here are the representatives of three different experiments.

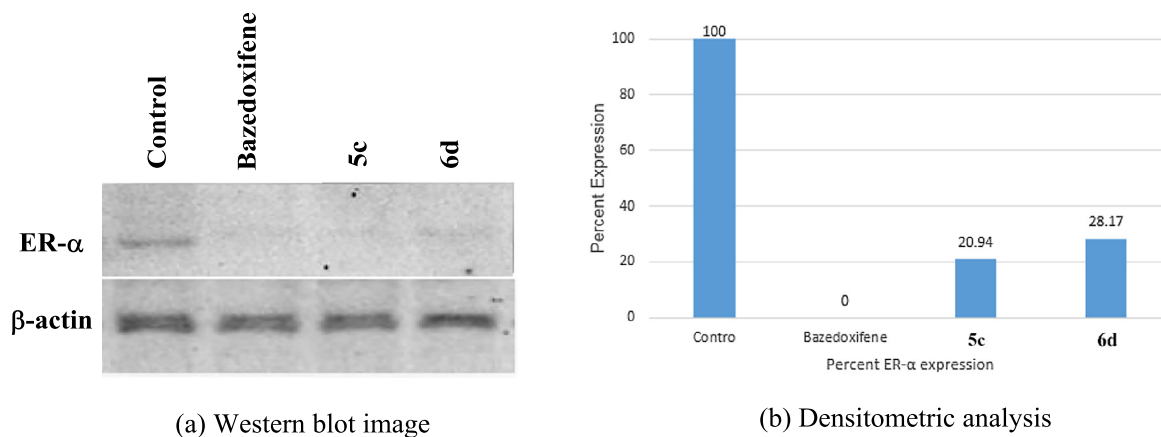


Fig. 7. Western blot analysis of endogenous ER- α protein in the T47D cells after treatment with bazedoxifene, 5c, and 6d. The cell line was incubated with 15, 5 and 10 μ M of bazedoxifene, 5c, and 6d respectively for 48 h. Data were normalized with β -actin as an internal control, the results shown here are the representatives of three different experiments.

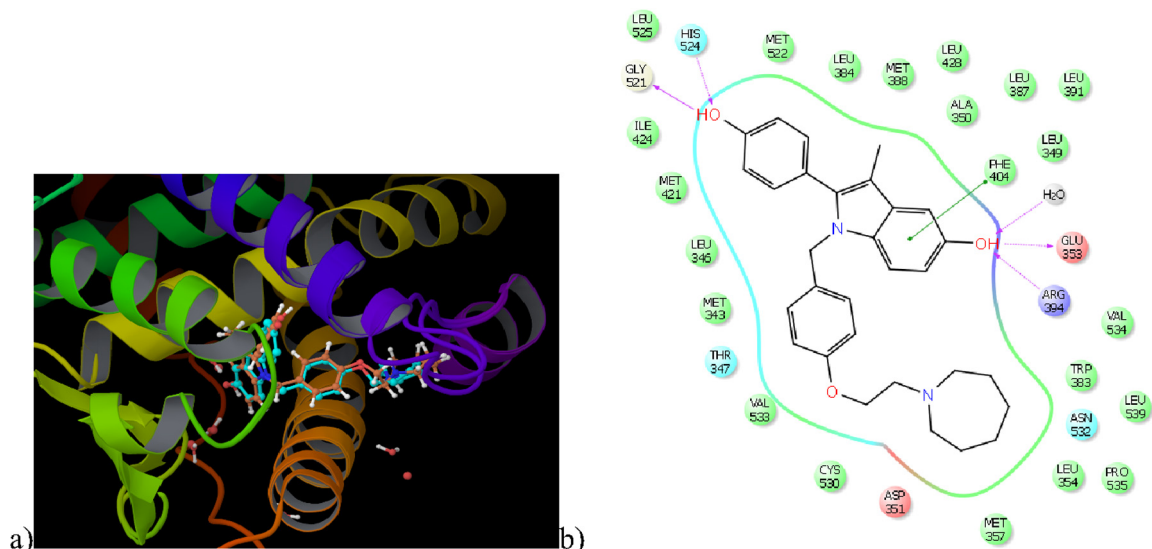


Fig. 8. (a) Superposition of the docked structure of bazedoxifene (blue) with the recrystallized experimental pose of bazedoxifene (orange) in 4X13 with 0.02 Å rmsd (b) Bazedoxifene ligand interaction diagram at the receptor site of ER- α .

Phe 404 (Fig. 9b, d). In addition, **5c** and **6d** were able to form van der Waals contacts with Met 343, Leu 346, Leu 349, Leu 354, Trp 383, Met 388, Met 421, Ile 424, Leu 428, Met 522, Leu 525, Cys 530, Val 533 and Pro 535 which were like the amino acid residues present in the ligand interaction diagram of bazedoxifene. This further signifies that compound was able to occupy the binding cavity in an antagonistic confirmation analogous to bazedoxifene. Thereby, indicating that compounds **5c** and **6d** upon binding to the active site of ER- α by extensive H-bond and van der Waals contacts causes a reduction in its expression.

The development of effective drugs for the treatment of hormone-dependent cancer is emerging as an important field of research in medicinal chemistry. The major strategies for hormonal therapy are to block the estrogens signaling pathways. The molecular docking in addition to the anti-proliferative activity and binding affinity illuminated some key structural aspects of the compound for targeting BC. The binding cavity of ER- α is narrow and lined by hydrophobic amino acids. The compound must possess a lipophilic character for binding successfully to the receptor. Hence, the structure-activity relationship revealed some interesting findings. I was found that compounds having

alkyl substituent as in case of **5a**, **5b**, **5c**, **6a**, **6b**, **6c**, and **6d** were found to be active at both cellular and receptor level as they can effectively enter the narrow cavity of the receptor and can form H-bonding/Van der Waals contact at the receptor site. On the contrary compound, **5e** which was devoid of any alkyl substituent was neither having anti-proliferative activity nor ER- α binding affinity. Another noteworthy finding was that the presence of bulky aryl groups such as phenyl and chloro-phenyl and as in case of compounds **5d**, **6e**, **6f** and **6j** reduces the activity of the compound. This can be due to restricted accesses of the compound to the binding cavity of ER- α , thereby, reducing the bioactivity. In addition, presence of heteroaryl side chains as in compounds **5f**, **6g**, **6h**, **6i**, **6k**, and **6l** adds an additional factor of H-bonding at the receptor site attributed to the heteroatom. The enhanced bonding at the receptor site counters the steric hindrance and hence improves the interaction at the receptor site. Biological activity and *in silico* investigation imply that anticancer potential of **5c** and **6d** was supported by strong binding affinity and confirmation to ER- α of these compounds similar to bazedoxifene which leads to reduced protein and mRNA expression. Hence, **5c** and **6d** can be identified as a

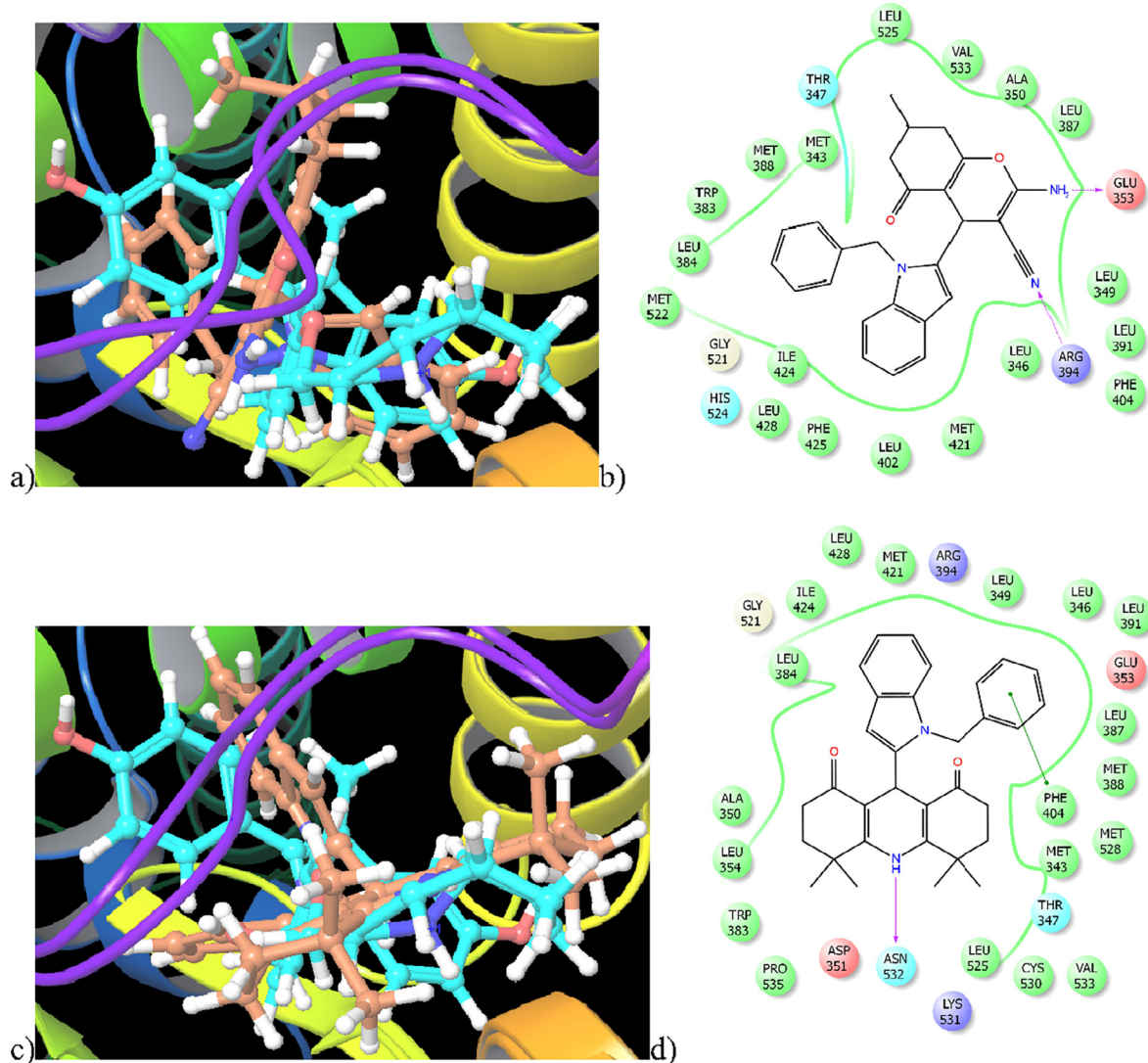


Fig. 9. (a) Superposition of bazedoxifene (brown) with compound **5c** (blue) at receptor site (b) ligand interaction diagram of compound **5c** (c) Superposition of bazedoxifene (brown) with compound **6d** (blue) at receptor site (d) ligand interaction diagram of compound **6d**. (Green outline corresponds to Van der Waals contacts, cyan outline polar interactions, pink arrow pointer H-bond interaction, green pointers π - π stacking).

potential lead molecule which might be of therapeutic importance for BC treatment.

3. Conclusion

In summary, herein we have described the design, synthesis and *in vitro* biological evaluation of novel indole derivatives for targeting ER- α . Indole based chromene and dihydropyridine derivatives were developed, and the combinatorial library was generated, screened by favorable drug-like ADME characteristics, docking profile and synthetic accessibility. All the synthesized derivatives were evaluated for the antiproliferative activity, cytotoxicity, and ER- α binding affinity. From these studies, it was found that methyl and dimethyl substituted compounds were more active than aryl substituted compounds. Compounds **5c** and **6d** were showing most promising antiproliferative and ER- α binding affinity. Therefore, **5c** and **6d** were forwarded for gene expression studies. CLSM experiment indicated that resultant antiproliferative activity of the compounds on T47D cells line was probably due to the accumulation of compound in the nucleoplasm, cytoplasm, and biomembrane. From the semi-quantitative RT-PCR and Western blotting, it was found that compounds **5c** and **6d** were able to decrease the mRNA and protein expression of the target ER- α , thereby reducing the ER- α activity. The result obtained the study were encouraging considering that compound **5c** and **6d** represents an example of indole derivatives which could be used for the lead optimization studies and can be expanded for *in vivo* testing as a potent compound for the management of BC.

4. Experimental

4.1. Combinatorial library enumeration and ADME screening

A combinatorial library was generated with the use of the CombiGlide software [33] by an iterative combination of an in-house database of reagents substituting R₁ and R₂ group (Fig. 1) with core structures. The compounds were subjected to ADME filtering and the following criteria were applied for filtering the compounds with favorable profiles log octanol/water ratio (QPlog Po/w, limit: -2.0 to 6.5), QPlog hERG (limit: above-5.0), QPP Caco (acceptable value: poor ~25, great ~500(nm/s)) QPPMDCK (acceptable limit: poor ~25, great ~500(nm/s)), QPlogKhsa (limit: -1.5 to 1.5) and percent oral absorption.

4.2. Docking with ER- α

The 2D structure of ligands was constructed using the Maestro 9.6 software and saved in sdf format (standard data format). The 2D structures were converted to the 3D structure using the Ligprep module of Maestro 9.6. This module adds hydrogens and eliminates any discrepancies between bond length and angle. The 3-dimensional and X-ray structure coordinates of ER- α was obtained from protein data bank with PDB id code 4XI3 (www.rcsb.org). Protein preparation wizard of maestro 9.6 was used for protein preparation. Protein preparation begins with the application of Impact molecular mechanics program for correcting the bond orders, adding missing hydrogens and removing the crystallized waters that are not present in the active site. Docking procedure was performed using GLIDE (Grid-based Ligand Docking with Energetics) software 9.6. Docking score was taken into consideration for comparing the results, more the negative value of docking score more potent is the compound and indicates the more binding potential. Docking score has several components such as hydrogen bonds (H-bond), hydrophobic contacts (Lipo), van der-waals interactions (vdW), coulombic interactions (Coul), polar interactions in

the binding site (Site), metal binding terms (Metal), penalty for buried polar groups (BuryP) and freezing rotatable bonds (RotB).

$$G - \text{score} = \Delta H_{\text{bond}} + \Delta_{\text{Lipo}} + \Delta_{\text{Metal}} + \Delta_{\text{Site}} + 0.130\text{Coul} \\ + 0.065\text{vdW} - \Delta_{\text{BuryP}} - \Delta_{\text{RotB}}$$

4.3. Chemistry

4.3.1. Chemistry

Starting materials and solvents were purchased from commercial suppliers and used without further purification. Reaction progress was monitored by TLC using silica gel 60 F254 (0.040e0.063 mm) with detection by UV. Silica gel 60–120 and 200–400 was used for column chromatography and flash chromatography respectively. Yields refer to purified materials and are not optimized. ¹H NMR and ¹³C NMR spectra were recorded on a Jeol 400 MHz and Bruker 400 MHz spectrometer using the residual signal of the deuterated solvent as internal standard. Splitting patterns are described as singlet (s), doublet (d), triplet (t) and broad (br); chemical shifts (d) are given in ppm. High-resolution mass spectra (HRMS) were recorded on a Q-ToF Micro Waters. Melting points were recorded on Stuart melting point apparatus (SMP-30) with open glass capillary tube and were uncorrected.

4.3.2. General procedure for the synthesis of intermediates **2**, **3** and **4**

Potassium hydroxide (4 mmol) was stirred in dried dimethyl sulfoxide (25 mL) for 10 min in a round-bottom flask. Ethyl 1H-indole-2-carboxylate **1** (1 mmol) was added to the solution, and the mixture was stirred for 0.5 h. Benzyl bromide (1.3 mmol) was added to the stirring mixture. After the completion of the reaction (1.5 h) as monitored by TLC, the reaction mixture was cooled to 0 °C. The product was extracted with ethyl acetate; the organic layer was washed using brine solution (40 mL). The combined organic layer was dried over anhydrous sodium sulfate, filtered, concentrated and was purified by flash column chromatography (petroleum ether: ethyl acetate = 9: 1, v/v) on silica gel (200–400) to get pure compound **2** with 95% yield.

For the synthesis of **3**, lithium aluminum hydride (2 mmol) was stirred in dry THF at 0 °C. Then **2** (1 mmol) was dissolved in THF and added dropwise to the solution of lithium aluminum hydride at 0 °C. Then, the mixture was slowly warmed to room temperature till the completion (0.5 h) of reaction as monitored by TLC. It was then cooled to 0 °C, 10% aqueous sodium hydroxide (20 mL) and 40 mL of water were added successively. The reaction mixture was allowed to stir for 0.5 h, filtered through Celite and washed with dry ethyl acetate, dried over anhydrous sodium sulfate, concentrated and purified by flash column chromatography (petroleum ether:ethyl acetate = 8:2, v/v) on silica gel (200–400) to get pure compound **3** with 98% yield.

For the synthesis of **4**, compound **3** (1 mmol) was dissolved in dry CH₂Cl₂ (25 mL) was stirred briefly. Activated manganese dioxide (7.3 mmol) was added, stirred at room temperature for 4 h. Another portion of activated manganese dioxide (5.9 mmol) was added and stirred at room temperature for 0.5 h. After completion of the reaction, as monitored by TLC, the reaction mixture was filtered through Celite and washed with ethyl acetate, concentrated and purified by flash chromatography (petroleum ether:ethyl acetate 9.5:0.5, v/v) on silica gel (200–400) to afford pure compound **4** with 70% yield. The structure of the compounds **2**, **3** and **4** were confirmed by comparing the spectroscopic data with the reported data.

4.3.3. General procedure for the synthesis of compounds **5a–f**

For the synthesis of **5a–f**, a mixture of compound **4** (1 mmol), corresponding dimedone (1 mmol) and malononitrile (1 mmol)

was refluxed with stirring for 12 h and was monitored for completion using TLC. The reaction was generally completed in 12–15 h. After the completion of the reaction, excess of ethanol was removed under reduced pressure. The product was extracted using ethyl acetate and organic layer was washed with distilled water. The combined organic layer was dried over anhydrous sodium sulfate, filtered, concentrated and purified by flash column chromatography (petroleum ether:ethyl acetate = 9:1, v/v) on silica gel (200–400) to afford compounds **5a–f** in 50–70% yields. The structures were confirmed by NMR and HRMS.

4.3.3.1. 2-amino-4-(1-benzyl-1H-indol-2-yl)-7,7-dimethyl-5-oxo-5,6,7,8-tetrahydro-4H-chromene-3-carbonitrile (5a). yellow solid; yield 50%; mp 191–193 °C; ¹H NMR (400 MHz, CDCl₃) δ 7.52–7.50 (1H, m), 7.30–7.26 (2H, m), 7.22–7.18 (1H, m), 7.16–7.14 (1H, d, *J* = 8 Hz), 7.11–7.09 (2H, m), 7.07–7.02 (2H, m), 6.30 (1H, s), 5.73–5.53 (2H, m), 4.69 (2H, s), 4.63 (1H, s), 2.31–2.30 (2H, m), 2.17–2.13 (1H, m), 2.05–2.01 (1H, m), 1.04 (3H, s), 1.01 (3H, s). ¹³C NMR (100 MHz, CDCl₃) δ 196.42, 161.77, 158.05, 142.52, 137.95, 137.30, 128.77 (2C), 127.87, 127.23, 126.32 (2C), 121.62, 120.36, 119.82, 118.72, 113.09, 110.16, 101.44, 61.60, 50.56, 47.03, 40.68, 32.18, 28.42, 28.20, 27.56. HRMS (ESI): *m/z* calcd for C₂₇H₂₆N₃O₂⁺ [M + H]⁺ 424.2025; found: 424.2023.

4.3.3.2. 2-amino-4-(1-benzyl-1H-indol-2-yl)-8,8-dimethyl-5-oxo-5,6,7,8-tetrahydro-4H-chromene-3-carbonitrile (5b). yellow solid; yield 69%; mp 116–118 °C; ¹H NMR (400 MHz, DMSO-*d*₆) δ 7.53–7.51 (1H, m), 7.29–7.25 (2H, m), 7.22–7.18 (1H, m), 7.14–7.12 (1H, m), 7.10–7.03 (4H, m), 6.31–6.25 (1H, m), 5.73–5.52 (2H, m), 4.69 (2H, s), 4.63 (1H, s), 2.49–2.46 (1H, m), 2.38–2.30 (1H, m), 1.78–1.73 (1H, m), 1.72–1.57 (1H, m), 1.04 (3H, s), 1.03 (3H, s). ¹³C NMR (100 MHz, CDCl₃) δ 196.20, 161.53, 158.01, 142.71, 138.00, 137.31, 128.75 (2C), 127.92, 127.19, 126.25 (2C), 121.51, 120.32, 119.75, 118.65, 112.45, 110.22, 101.34, 61.77, 47.04, 40.55, 34.79, 33.28, 28.04, 25.95, 24.37. HRMS (ESI): *m/z* calcd for C₂₇H₂₆N₃O₂⁺ [M + H]⁺ 424.2025; found: 424.2027.

4.3.3.3. 2-amino-4-(1-benzyl-1H-indol-2-yl)-7-methyl-5-oxo-5,6,7,8-tetrahydro-4H-chromene-3-carbonitrile (5c). pale yellow solid; yield 70%; mp 203–204 °C; ¹H NMR (400 MHz, DMSO-*d*₆) δ 7.52–7.51 (1H, d, *J* = 8 Hz), 7.30–7.25 (2H, m), 7.24–7.18 (1H, m), 7.16–7.14 (1H, d, *J* = 8 Hz), 7.09–7.02 (4H, m), 6.31–6.30 (1H, m), 5.73–5.51 (2H, m), 4.64 (1H, s), 4.58 (2H, s), 2.53–2.44 (1H, m), 2.36–2.18 (2H, m), 2.03–1.79 (2H, m), 1.04–1.03 (3H, m). ¹³C NMR (100 MHz, DMSO-*d*₆) δ 196.10, 163.06, 157.91, 142.31, 137.91, 137.38, 128.68 (2C), 127.78, 127.17, 126.19 (2C), 121.62, 120.28, 119.81, 118.43, 114.13, 110.11, 101.44, 62.18, 46.96, 44.83, 35.06, 34.80, 27.36, 20.58. HRMS (ESI): *m/z* calcd for C₂₆H₂₄N₃O₂⁺ [M + H]⁺ 410.1869; found: 410.1868.

4.3.3.4. 2-amino-4-(1-benzyl-1H-indol-2-yl)-5-oxo-7-phenyl-5,6,7,8-tetrahydro-4H-chromene-3-carbonitrile (5d). bright yellow solid; yield 64%; mp 141–142 °C; ¹H NMR (400 MHz, CDCl₃) δ 7.57–7.51 (1H, m), 7.35–7.24 (6H, m), 7.16–7.14 (2H, m), 7.10–7.04 (5H, m), 6.42–6.31 (1H, m), 5.74–5.54 (2H, m), 4.72 (1H, s), 4.65 (2H, s), 3.37–2.93 (1H, m), 2.71–2.63 (2H, m), 2.57–2.45 (2H, m). ¹³C NMR (100 MHz, CDCl₃) δ 195.27, 162.87, 158.03, 141.97, 141.68, 138.11, 137.54, 129.06 (2C), 128.91 (2C), 128.86, 127.88, 127.50, 126.70 (2C), 126.20 (2C), 121.85, 120.48, 120.01, 118.44, 114.40, 110.19, 101.96, 62.22, 47.00, 43.79, 38.68, 37.64, 27.96. HRMS (ESI): *m/z* calcd for C₃₁H₂₆N₃O₂⁺ [M + H]⁺ 472.2025; found: 472.2028.

4.3.3.5. 2-amino-4-(1-benzyl-1H-indol-2-yl)-5-oxo-5,6,7,8-tetrahydro-4H-chromene-3-carbonitrile (5e). red solid; yield 53%; mp 189–190 °C; ¹H NMR (400 MHz, DMSO-*d*₆) δ 7.53–7.52 (1H, m),

7.30–7.25 (2H, m), 7.23–7.19 (1H, m), 7.16–7.14 (1H, d, *J* = 8 Hz), 7.10–7.02 (4H, m), 6.32–6.31 (1H, m), 5.74–5.52 (2H, m), 4.65 (1H, s), 4.59 (2H, s), 2.54–2.44 (1H, m), 2.37–2.32 (1H, m), 2.24–2.18 (1H, m), 2.04–1.80 (2H, m), 1.41–1.24 (1H, m); ¹³C NMR (100 MHz, DMSO-*d*₆) δ 196.12, 163.08, 157.93, 142.33, 137.93, 137.34, 128.70 (2C), 127.80, 127.19, 126.21 (2C), 121.64, 120.30, 119.83, 118.45, 114.15, 110.13, 100.23, 62.20, 46.98, 35.08, 28.25, 27.38, 20.60. HRMS (ESI): *m/z* calcd for C₂₅H₂₁N₃O₂⁺ [M]⁺ 395.1634; found: 395.1633.

4.3.3.6. 2-amino-7-(benzo[d][1,3]dioxol-5-yl)-4-(1-benzyl-1H-indol-2-yl)-5-oxo-5,6,7,8-tetrahydro-4H-chromene-3-carbonitrile (5f). white solid; yield 69%; mp 234–235 °C; ¹H NMR (400 MHz, CDCl₃) δ 7.56–7.51 (1H, m), 7.32–7.23 (4H, m), 7.17–7.14 (1H, m), 7.10–7.03 (4H, m), 6.77–6.71 (1H, m), 6.64–6.54 (2H, m), 5.94 (2H, s), 5.74–5.51 (2H, m), 4.70 (1H, s), 4.56 (2H, s), 3.30–2.86 (1H, m), 2.66–2.59 (2H, m), 2.53–2.39 (1H, m), 2.24–2.04 (1H, m). ¹³C NMR (100 MHz, CDCl₃) δ 195.34, 161.83, 157.64, 148.09, 146.85, 141.15, 138.06, 137.60, 135.63, 128.91 (2C), 127.78, 127.28, 126.16 (2C), 121.78, 120.50, 119.92, 119.77, 119.84, 118.30, 109.97, 108.57, 107.02, 102.30, 101.27, 62.09, 46.94, 44.01, 38.54, 34.93, 28.21. HRMS (ESI): *m/z* calcd for C₃₂H₂₆N₃O₄⁺ [M + H]⁺ 516.1923; found: 516.1924.

4.3.4. General procedure for the synthesis of compounds **6a–l**

For the synthesis of **6a–l**, a mixture of compound **4** (1 mmol), corresponding dimedone (2 mmol), ammonium acetate (1 mmol) and ascorbic acid (10 mol%) was stirred for at 10 °C and was monitored for completion using TLC. The reaction was generally completed in 9–10 h. After the completion of the reaction, excess of ethanol was removed under reduced pressure. The product was extracted using ethyl acetate and organic layer was washed with distilled water. The combined organic layer was dried over anhydrous sodium sulfate, filtered, concentrated and purified by isocratic flash column chromatography (petroleum ether:ethyl acetate = 9:1, v/v) on silica gel (200–400) to afford compounds **6a–l** in 60–70% yields. The structures were confirmed by NMR and HRMS.

4.3.4.1. 9-(1-benzyl-1H-indol-2-yl)-3,3,6-trimethyl-3,4,6,7,9,10-hexahydroacridine-1,8(2H,5H)-dione (6a). off white solid; yield 77%; mp 175–177 °C; ¹H NMR (400 MHz, CDCl₃) δ 12.17 (1H, s), 7.58–7.57 (1H, m), 7.30–7.27 (4H, m), 7.18–7.16 (2H, m), 6.93–6.89 (2H, m), 6.48 (1H, s), 5.55 (1H, s), 5.13 (2H, s), 2.49–2.40 (2H, m), 2.32–2.27 (2H, m), 2.20–2.15 (2H, m), 2.05–2.01 (2H, m), 1.92–1.78 (1H, m), 1.05 (6H, s), 1.04–1.03 (3H, m). ¹³C NMR (100 MHz, CDCl₃) δ 191.25, 190.43, 146.55 (2C), 138.23, 137.85, 136.94, 128.23 (2C), 127.76, 125.77 (2C), 125.70, 121.63, 120.36, 119.94, 115.43 (2C), 109.59, 102.81, 47.98, 47.03, 46.16, 40.05, 39.35, 38.56, 37.11, 27.75, 22.77, 22.69, 20.83. HRMS (ESI): *m/z* calcd for C₃₁H₃₄N₂O₂⁺ [M + 2H]⁺ 466.2620; found: 466.2629.

4.3.4.2. 9-(1-benzyl-1H-indol-2-yl)-3,3,6,6-tetramethyl-3,4,6,7,9,10-hexahydroacridine-1,8(2H,5H)-dione (6b). yellow solid; yield 45%; mp 220–222 °C; ¹H NMR (400 MHz, CDCl₃) δ 12.16 (1H, s), 7.57 (1H, m), 7.27 (1H, m), 7.25 (1H, m), 7.19 (2H, m), 7.08 (1H, m), 7.06 (2H, m), 6.95 (1H, m), 6.48 (1H, s), 5.13 (2H, s), 4.13 (1H, s), 2.20 (4H, s), 1.25 (4H, s), 0.95 (12H, s); ¹³C NMR (100 MHz, CDCl₃) δ 190.10 (2C), 144.88 (2C), 138.21, 137.84, 136.93, 128.91 (2C), 128.21, 127.08 (2C), 125.80, 121.66, 120.37, 119.93, 115.41 (2C), 109.58, 102.79, 47.02, 46.85 (2C), 46.23 (2C), 31.97, 29.81, 28.45, 27.92, 27.73, 27.40, 22.76. HRMS (ESI): *m/z* calcd for C₃₂H₃₆N₂O₂⁺ [M + 2H]⁺ 480.2777; found: 480.2717.

4.3.4.3. 9-(1-benzyl-1H-indol-2-yl)-3,6-dimethyl-3,4,6,7,9,10-hexahydroacridine-1,8(2H,5H)-dione (6c). off white solid; yield 55%; mp

190–193 °C; ¹H NMR (400 MHz, CDCl₃) δ 12.45 (1H, s), 7.57 (1H, m), 7.49 (1H, m), 7.24 (1H, m), 7.08 (2H, m), 7.01 (1H, m), 6.96 (2H, m), 6.90 (1H, m), 6.49 (1H, s), 5.54 (2H, s), 5.15 (1H, s), 2.41 (4H, m), 1.95 (4H, m), 1.30–1.22 (2H, m), 0.90 (6H, m); ¹³C NMR (100 MHz, CDCl₃) δ 191.26 (2C), 147.61 (2C), 141.86, 137.78, 137.15, 128.82 (2C), 128.70, 127.08 (2C), 125.66, 121.57, 120.31, 119.93, 116.79 (2C), 109.65, 102.73, 54.03, 47.06 (2C), 40.97 (2C), 26.79 (2C), 26.67 (2C), 20.54. HRMS (ESI): *m/z* calcd for C₃₀H₃₂N₂O₂+ [M + 2H]⁺ 452.2464; found: 452.2461.

4.3.4.4. 9-(1-benzyl-1H-indol-2-yl)-4,4,5,5-tetramethyl-3,4,6,7,9,10-hexahydroacridine-1,8(2H,5H)-dione (**6d**). light yellow solid; yield 54%; mp 170–172 °C; ¹H NMR (400 MHz, CDCl₃) δ 12.69 (1H, s), 7.58–7.57 (1H, m), 7.56–7.55 (1H, m), 7.52–7.49 (1H, m), 7.30–7.27 (2H, m), 7.21–7.19 (1H, m), 7.10–7.08 (2H, m), 7.06–7.05 (1H, m), 7.03–7.02 (1H, m), 5.49 (2H, s), 4.94 (1H, s), 1.38 (4H, m), 1.23 (4H, m), 1.07 (12H, m). ¹³C NMR (100 MHz, CDCl₃) δ 196.62 (2C), 166.77 (2C), 142.22, 137.76, 137.52, 129.14, 128.79 (2C), 127.20, 125.59 (2C), 121.49, 120.30, 119.88, 115.14 (2C), 109.84, 102.51, 51.07, 38.17 (2C), 35.63 (2C), 33.25 (2C), 28.03, 26.24 (2C), 24.43 (2C). HRMS (ESI): *m/z* calcd for C₃₂H₃₆N₂O₂+ [M + 2H]⁺ 480.2777; found: 480.2719.

4.3.4.5. 9-(1-benzyl-1H-indol-2-yl)-3,6-diphenyl-3,4,6,7,9,10-hexahydroacridine-1,8(2H,5H)-dione (**6e**). light brown solid; yield 40%; mp 110–112 °C; ¹H NMR (400 MHz, CDCl₃) δ 12.90 (1H, s), 7.64–7.62 (1H, m), 7.60–7.58 (1H, m), 7.33–7.32 (4H, m), 7.29–7.26 (8H, m), 7.20–7.18 (2H, m), 7.14–7.10 (2H, m), 7.04–6.99 (1H, m), 6.62 (1H, s), 5.26 (2H, s), 3.30 (1H, s), 2.54 (4H, m), 1.63–1.55 (2H, m), 1.22 (4H, m); ¹³C NMR (100 MHz, CDCl₃) δ 190.59 (2C), 150.14 (2C), 142.07 (2C), 140.07, 137.90, 136.86, 128.88 (6C), 127.22, 126.75 (6C), 125.72 (3C), 121.77, 120.39, 120.10, 116.57 (2C), 109.94, 102.92, 47.16, 41.05 (2C), 39.97 (2C), 37.03 (2C), 28.43. HRMS (ESI): *m/z* calcd for C₄₀H₃₆N₂O₂+ [M + 2H]⁺ 576.2777; found: 576.2721.

4.3.4.6. 9-(1-benzyl-1H-indol-2-yl)-3,6-bis(4-chlorophenyl)-3,4,6,7,9,10-hexahydroacridine-1,8(2H,5H)-dione (**6f**). yellow solid; yield 50%; mp 122–124 °C; ¹H NMR (400 MHz, CDCl₃) δ 12.86 (1H, s), 7.61–7.60 (1H, m), 7.31–7.24 (8H, m), 7.19–7.09 (2H, m), 7.02–6.97 (6H, m), 6.58–6.45 (1H, m), 5.67 (1H, s), 5.23 (2H, s), 2.64–2.55 (4H, m), 1.63–1.41 (2H, m), 1.29–1.20 (4H, m). ¹³C NMR (100 MHz, CDCl₃) δ 190.23 (2C), 150.29 (2C), 142.14 (2C), 140.44, 137.85, 136.66, 132.94 (2C), 129.01 (6C), 128.23, 128.08 (6C), 125.73, 121.84, 120.38, 120.15, 116.56 (2C), 109.92, 102.93, 47.12, 40.87 (2C), 39.85 (2C), 36.43 (2C), 28.38. HRMS (ESI): *m/z* calcd for C₄₀H₃₄Cl₂N₂O₂+ [M + 2H]⁺ 644.1997; found: 644.1864.

4.3.4.7. 9-(1-benzyl-1H-indol-2-yl)-3,6-di(furan-2-yl)-3,4,6,7,9,10-hexahydroacridine-1,8(2H,5H)-dione (**6g**). brown solid; yield 95%; mp 142–144 °C; ¹H NMR (400 MHz, CDCl₃) δ 12.84 (1H, s), 7.60–7.56 (1H, m), 7.31–7.24 (4H, m), 7.18–7.07 (3H, m), 6.97–6.96 (2H, m), 6.78–6.72 (2H, m), 6.56–6.51 (4H, m), 5.93 (2H, s), 5.28 (1H, s), 2.59–2.43 (4H, m), 1.23–1.20 (4H, m), 0.86–0.82 (2H, m). ¹³C NMR (100 MHz, CDCl₃) δ 191.29 (2C), 156.33 (2C), 152.48 (2C), 142.77 (2C), 138.60, 138.52, 137.56, 129.59 (2C), 127.92, 127.45 (2C), 126.42, 122.47, 121.09, 120.80, 117.28 (2C), 110.64 (2C), 110.38 (2C), 109.06, 103.62, 53.89, 47.86 (2C), 41.75 (2C), 40.67, 37.73, 29.13. HRMS (ESI): *m/z* calcd for C₃₆H₃₀N₂O₄+ [M]⁺ 554.2206; found: 554.2231.

4.3.4.8. 3,6-bis(benzo[d][1,3]dioxol-5-yl)-9-(1-benzyl-1H-indol-2-yl)-3,4,6,7,9,10-hexahydroacridine-1,8(2H,5H)-dione (**6h**). off white solid; yield 55%; mp 190–193 °C; ¹H NMR (400 MHz, CDCl₃) δ 12.86 (1H, s), 7.31–7.25 (6H, m), 7.09–7.08 (2H, m), 7.01–6.98 (1H, m), 6.95–6.93 (1H, m), 6.91–6.89 (1H, m), 6.55 (1H, s), 6.27

(4H, s), 5.94 (2H, s), 5.62–5.53 (2H, m), 5.20 (2H, s), 5.06 (1H, s), 2.72–2.66 (4H, m), 1.26–1.20 (4H, m), 0.86–0.76 (2H, m). ¹³C NMR (100 MHz, CDCl₃) δ 190.07 (2C), 155.33 (2C), 141.79 (2C), 138.15, 137.98, 137.74 (2C), 137.70 (2C), 136.66, 128.90 (2C), 127.47, 125.61 (2C), 125.51, 121.79, 121.69, 120.38 (2C), 120.08, 116.51 (2C), 110.14 (2C), 109.63 (2C), 109.79, 104.80 (2C), 102.92, 47.03, 38.48 (2C), 37.44 (2C), 30.88 (2C), 28.35. HRMS (ESI): *m/z* calcd for C₄₂H₃₆N₂O₆+ [M + 2H]⁺ 664.2573; found: 664.2525.

4.3.4.9. 9-(1-benzyl-1H-indol-2-yl)-3-(furan-2-yl)-6-phenyl-3,4,6,7,9,10-hexahydroacridine-1,8(2H,5H)-dione (**6i**). light brown solid; yield 80%; mp 135–137 °C; ¹H NMR (400 MHz, CDCl₃) δ 12.85 (1H, s), 7.32–7.24 (10H, m), 7.10–7.07 (3H, m), 6.99–6.95 (2H, m), 6.28 (1H, s), 6.03–5.95 (1H, m), 5.68–5.53 (1H, m), 5.22 (2H, s), 5.10 (1H, s), 2.55–2.49 (4H, m), 1.26–1.21 (4H, m), 0.86–0.81 (2H, m). ¹³C NMR (100 MHz, CDCl₃) δ 190.42, 190.15, 155.46, 151.61 (2C), 141.90, 140.18, 137.73, 137.65, 136.69, 128.88 (2C), 128.78 (2C), 128.72, 127.05 (2C), 126.58 (2C), 125.55 (2C), 121.60, 120.22, 119.93, 116.41 (2C), 109.77 (2C), 109.51, 102.75, 51.07, 46.99, 46.85, 40.88, 39.80, 36.86, 29.69, 28.26. HRMS (ESI): *m/z* calcd for C₃₈H₃₄N₂O₃+ [M + 2H]⁺ 566.2569; found: 566.2534.

4.3.4.10. 9-(1-benzyl-1H-indol-2-yl)-3-(4-chlorophenyl)-6-phenyl-3,4,6,7,9,10-hexahydroacridine-1,8(2H,5H)-dione (**6j**). yellow solid; yield 92%; mp 117–119 °C; ¹H NMR (400 MHz, CDCl₃) δ 12.84 (1H, s), 7.61–7.56 (1H, m), 7.31–7.22 (10H, m), 7.13–7.08 (4H, m), 7.02–6.97 (4H, m), 5.67 (1H, s), 5.23 (2H, s), 2.65–2.58 (4H, m), 2.55–2.47 (4H, m), 1.57–1.42 (2H, m). ¹³C NMR (100 MHz, CDCl₃) δ 189.07, 188.83, 149.13 (2C), 140.98, 139.84, 139.28, 136.70, 135.50, 131.78, 127.85 (4C), 127.77 (2C), 127.07, 126.92 (4C), 126.61 (2C), 124.57 (2C), 120.68, 119.22, 119.00, 115.40 (2C), 108.76, 101.77, 52.96, 45.96, 45.83, 39.72, 38.69, 35.64, 35.28, 27.22. HRMS (ESI): *m/z* calcd for C₄₀H₃₅ClN₂O₂+ [M + 2H]⁺ 610.2387; found: 610.2374.

4.3.4.11. 9-(1-benzyl-1H-indol-2-yl)-3-(4-chlorophenyl)-6-(furan-2-yl)-3,4,6,7,9,10-hexahydroacridine-1,8(2H,5H)-dione (**6k**). off white solid; yield 55%; mp 190–193 °C; ¹H NMR (400 MHz, CDCl₃) δ 12.84 (1H, s), 7.61–7.55 (1H, m), 7.30–7.25 (9H, m), 7.02–6.95 (4H, m), 6.56 (1H, s), 6.34–6.28 (2H, m), 5.22 (2H, s), 5.09 (1H, s), 2.75–2.65 (4H, m), 1.59–1.52 (2H, m), 0.87–0.82 (4H, m). ¹³C NMR (100 MHz, CDCl₃) δ 190.20, 189.94, 155.35 (2C), 146.56, 141.82, 141.79, 140.47, 136.64, 136.41, 132.91, 129.01 (2C), 128.91 (2C), 128.21 (2C), 128.05 (2C), 127.76, 125.75, 121.81, 120.38, 120.12, 116.54 (2C), 110.15 (2C), 109.85, 102.93, 46.98, 40.87, 39.86, 38.55, 37.40, 30.94, 29.83, 28.38. HRMS (ESI): *m/z* calcd for C₃₈H₃₃ClN₂O₃+ [M + 2H]⁺ 600.2180; found: 600.2131.

4.3.4.12. 3-(benzo[d][1,3]dioxol-5-yl)-9-(1-benzyl-1H-indol-2-yl)-6-(4-chlorophenyl)-3,4,6,7,9,10-hexahydroacridine-1,8(2H,5H)-dione (**6l**). yellow solid; yield 45%; mp 140–142 °C; ¹H NMR (400 MHz, CDCl₃) δ 12.82 (1H, s), 7.61–7.59 (1H, m), 7.33–7.25 (7H, m), 7.11–7.09 (2H, m), 7.08–6.97 (4H, m), 6.75–6.73 (1H, m), 6.57 (2H, s), 5.94 (2H, s), 5.65 (1H, s), 5.23 (2H, s), 2.64–2.58 (4H, m), 2.50–2.44 (4H, m), 1.33–1.21 (2H, m); ¹³C NMR (100 MHz, CDCl₃) δ 195.23, 195.00, 157.52 (2C), 147.97, 146.73, 141.75, 141.04, 137.95, 137.48, 135.51, 135.45, 128.80 (2C), 128.72 (2C), 127.67, 127.25, 127.16 (2C), 126.05 (2C), 121.67, 120.39, 119.81, 119.72, 118.19 (2C), 110.04, 109.85, 108.45, 102.19, 101.16, 46.83, 43.95, 43.89, 38.42, 37.33, 34.82, 32.88, 28.10. HRMS (ESI): *m/z* calcd for C₄₁H₃₅ClN₂O₄+ [M + 2H]⁺ 654.2285; found: 654.2275.

4.4. Biological assay methods

The biological methodologies and techniques utilized herein corresponds to our recent published reports with slight modifications [20,21].

4.4.1. Culturing and maintaining of cancer cell line

Human BC cell line T47D were procured from National Centre for Cell Sciences (NCCS) Pune. T47D cells were grown in the Roswell Park Memorial Institute-1640 (RPMI-1640) medium supplemented with 10% heat inactivated (30 min at 56 °C) FBS (Fetal Bovine Serum), 1X penicillin and streptomycin in a tissue culture flask at 37 °C in a humidified atmosphere of 5% CO₂ incubator. At 70–80% confluence the cells were trypsinized using 1X trypsin-EDTA and sub-cultured in a new sterile tissue culture flask for further experiments.

4.4.2. Anti-proliferative activity

The anti-proliferative activity of the compounds was evaluated using the MTT (3-(4,5-dimethylthiazol-2-yl)-2,5-diphenyltetrazolium bromide) assay. It is a colorimetric assay for assessing cell metabolic activity. Viable cells with active metabolism convert the MTT into a purple colored formazan product with an absorbance maximum near 570 nm. When cells die, they lose the ability to convert MTT into formazan, thus color formation serves as a useful and convenient marker of only the viable cells. Human BC cell line T47D were seeded in 96 wells plate at cell density 1x10⁴ per well and after 24 h, cells were treated with different concentration of synthesized compounds (1, 5, 25 μM) and incubated for 48 h in FBS-free media. MTT solution (final concentration of MTT was 0.5 mg/ml) was added followed by incubation for 4 h at 37 °C. After 4 h; the purple color formazone crystals were solubilized using 100 μL of acidified DMSO with 0.6% acetic acid and absorbance was measured at both 570 nm and 620 nm. The absorbance reading is directly proportional to a number of living cells [54]. The cell viability of each group was calculated with their respective control. The Anti-proliferative experiment was performed in triplicate.

4.4.3. Human peripheral blood mononuclear cells (PBMCs) culture and MTT assay

Majority of the chemotherapeutic agents available having a side effect of inducing apoptosis in the normal cell along with the cancer cells. Therefore, in order to analyze the side effect of the compounds on the normal cells at higher concentrations, human PBMC was cultured and MTT assay was performed. Fresh blood was drawn from healthy individual as per the protocol no. CUPB/cc/14/IEC/4483 approved by Institutional Ethics Committee of Central University of Punjab, Bathinda. The protocol used was standard operating procedure, provided by Institutional Ethics Committee of Central University of Punjab according to guidelines issued by Indian Council of Medical Research (ICMR), Govt. of India. PBMC were isolated from whole blood discarding the RBCs (Red Blood Cells) after treatment with RBC lysis buffer. The PBMCs were counted on the automated cell counter (Invitrogen). The cells were then suspended in RPMI-1640 media supplemented with 10% fetal bovine serum (FBS), 1x antibiotic solution and incubated at 37 °C for 24 h in a humidified chamber of 5% CO₂. Approximately 10⁴ cells were seeded in each well of the 96 well plate. MTT assay was performed as described in Section 4.4.2. The cytotoxicity of the compounds was evaluated at 25, 50 and 100 μM concentration and the experiment was performed in triplicate.

4.4.4. Estrogen receptor competitive binding assay

A stock solution of each compound was serially diluted using DMSO, and the 40 μL of each concentration was transferred to the assay plate (Grenier, 384-well high volume flat bottom)

followed by adding 40 μL human recombinant ER-α/fluoromone TM complex solution. After mixing and allowing at least 2 h incubation at room temperature with light protection of the reagents. The fluorescence of each well was measured using the Synergy 2 multi-mode microplate reader (BioTek) with 535 nm excitation filters and 590 nm emission filters. Three controls were included in the assay: (1) assay maximum polarization control (40 μL of ER/fluoromone complex solution and 40 μL of ER green assay buffer with 4% DMSO, provides maximum polarization value for assay); (2) assay minimum polarization control (40 μL of ER/fluoromone complex solution and 40 μL of oestradiol (20 mM), provides bottom baseline); (3) free fluoromone tracer control (40 μL Fluoromone tracer and 40 μL of ER green assay buffer with 4% DMSO, provides absolute minimum polarization value). The polarization values were normalized to percent inhibition using the following equation.

$$I\% = (A_0 - A)/(A_0 - A_{100}) \times 100$$

I% = the percent inhibition, A₀ = Absorbance at 0% inhibition, A₁₀₀ = Absorbance at 100% inhibition, and A = observed Absorbance value.

The percent inhibition values are plotted against the concentration of test compounds and analyzed by a non-linear regression curve fitting. The concentration of the test compounds needed to displace half of the bound ligand equals IC₅₀ of the test compound.

4.4.5. Confocal microscopy

Cell imaging is an important technique for localisation of the compound inside the cell. As the ER is located in the plasma membrane, cytosol, and nucleoplasm, live cell imaging enables to track the compound and site of action. Cells were seeded in sterile glass coverslip at 5 × 10⁴ cells/ml in a 6 well plate. After 24 h of seeding the cells were treated with 5 and 15 μM of **5c** and **6d** for 48 h after that cells were washed with 1X PSB. After that cells were fixed with 2% formaldehyde solution for 10 min in the dark, again cells were washed thrice with 1X PBST. Then cells were mounted on glass cover by using mounting media. Cells were visualized an image was captured under an Olympus FV1200 Laser Scanning Microscopes fluorescence confocal microscope; the captured image was analyzed with Olympus Fluoview software of Olympus version 4.2a. The CLSM experiment was performed in duplicate.

4.4.6. Preparation of total cell lysates

To determine target specificity of the compounds, there is a need to establish the expression of target proteins. Cell lysates were prepared from both treated and untreated cells of T47D. Briefly, cells were first rinsed twice gently with ice-cold 1X PBS, then 300–500 μL of modified RIPA buffer [50 mM Tris-HCl (pH 7.4), 150 mM NaCl, 1 mM EDTA, 1% NP-40, and protease inhibitor cocktail (1 μL per 100 μL of lysis buffer)] was added per plate, kept on ice for 5 min, and cells were mechanically scraped using plastic cell scraper, and cell suspension was transferred into pre-cooled 1.5 mL microcentrifuge tube [55]. Following centrifugation, the pellet was re-suspended in the cell lysis buffer with intermediate vortexing every 5 min for 20 min at 4 °C. Then, the mixture was centrifuged at 12,000g for 20 min at 4 °C. The supernatant was collected in prechilled sterile microcentrifuge tubes and stored at –20 °C for further experiments. The concentration of total protein in this supernatant was estimated by using standard Bradford method with BSA as standard [56].

4.4.7. Western blot analysis

50 μg of total protein samples were resolved on 10% denaturation SDS-PAGE and transferred to a nitrocellulose membrane. Membranes were blocked for 1 h with 5% nonfat dry milk (NFD) in 1X PBST. All antibody dilutions were made in 2.5% NFD-PBST. Membranes were incubated (4 °C overnight) with primary

antibodies of rabbit α -ER- α (HC-20). Membranes were washed with PBST, incubated with horseradish peroxidase-conjugated secondary antibody (Invitrogen) for 1 h. The image was captured by using Bio-Rad ChemiDoc™ MP imaging system after applying enhanced chemiluminescence (Clarity™ Western ECL Substrate of Bio-Rad), and densitometric analysis was done using Image Lab™ software of Bio-Rad version 5.2. The Western blotting experiment was performed in triplicate.

4.4.8. Total RNA isolation and cDNA synthesis

Total RNA was isolated from T47D cells from both treated and untreated cells by using TRIzol® (Invitrogen) and followed the manufacturer instructions, and finally, RNA pellet was resuspended in nuclease-free water. Quality of isolated RNA was checked on NanoDrop 2000c (Thermo Scientific) followed by denaturing agarose gel. Traces of DNA contamination was removed by treating the total isolated RNA with DNA-free™ DNA Removal Kit (Invitrogen) and followed the manufacturer instructions. Again, the quality of DNA free RNA was checked, followed by synthesis of the first strand of cDNA by using the SuperScript™ IV First-Strand Synthesis System (Invitrogen) as per the instructions by the manufacturer.

4.4.9. Semi-quantitative RT-PCR

cDNA was used as a template for the PCR reaction with gene-specific primer pairs of ER- α (5' GTGCCTGGCTAGAGATCCTG 3', 3' GATGTGGGAGAGGATGAGGA 5') along with a housekeeping gene (GAPDH) as a loading control. The PCR product was separated on 1.2% agarose gel containing ethidium bromide (EtBr) along with 100 bp DNA ladder of Invitrogen (TrackIt™ 100 bp DNA ladder). The gel image was taken by using Bio-Rad Gel Doc™ XR system, and densitometric analysis was done using Image Lab™ software of Bio-Rad version 5.2. The RT-PCR experiment was performed in triplicate.

Acknowledgment

Authors are grateful to Department of Science and Technology, New Delhi, India for providing financial assistance during the work. Ramit Singla acknowledges CSIR-India for the award of SRF. Authors acknowledge Mr. Ashish Pandey of CIL in the Central University of Punjab, for outstanding work on CLSM. Authors are also thankful to the Honourable Vice-Chancellor for providing the necessary facilities at Central University of Punjab, Bathinda, India.

Appendix A. Supplementary material

Supplementary data associated with this article can be found, in the online version, at <https://doi.org/10.1016/j.bioorg.2018.04.002>.

References

- [1] M. Dutertre, C.L. Smith, Molecular mechanisms of selective estrogen receptor modulator (SERM) action, *J. Pharmacol. Exp. Ther.* 295 (2) (2000) 431–437.
- [2] K. Maruyama, M. Nakamura, S. Tomoshige, K. Sugita, M. Makishima, Y. Hashimoto, M. Ishikawa, Structure–activity relationships of bisphenol A analogs at estrogen receptors (ERs): discovery of an ER α -selective antagonist, *Bioorg. Med. Chem. Lett.* 23 (14) (2013) 4031–4036.
- [3] C. Yang, G. Xu, J. Li, X. Wu, B. Liu, X. Yan, M. Wang, Y. Xie, Benzothiofenones containing a piperazine side chain as selective ligands for the estrogen receptor α and their bioactivities in vivo, *Bioorg. Med. Chem. Lett.* 15 (5) (2005) 1505–1507.
- [4] S.J. Howell, S.R.D. Johnston, A. Howell, The use of selective estrogen receptor modulators and selective estrogen receptor down-regulators in breast cancer, *Best Practice Res.: Clin. Endocrinol. Metabolism* 18 (1) (2004) 47–66.
- [5] J.H. Pickar, B.S. Komm, Selective estrogen receptor modulators and the combination therapy conjugated estrogens/bazedoxifene: a review of effects on the breast, *Post Reproductive Health* 21 (3) (2015) 112–121.
- [6] S.L. Silverman, C. Christiansen, H.K. Genant, S. Vukicevic, J.R. Zanchetta, T.J. de Villiers, G.D. Constantine, A.A. Chines, Efficacy of bazedoxifene in reducing new vertebral fracture risk in postmenopausal women with osteoporosis: results from a 3-year, randomized, placebo-, and active-controlled clinical trial, *J. Bone Mineral Res.* 23 (12) (2008) 1923–1934.
- [7] M.D. Rinath, Jeselsohn, A Study of Palbociclib in Combination With Bazedoxifene in Hormone Receptor Positive Breast Cancer, 2017. <<https://clinicaltrials.gov/ct2/show/NCT02448771>>. (Accessed 9/7/2017).
- [8] A.K. Singh, V. Raj, S. Saha, Indole-fused azepines and analogues as anticancer lead molecules: privileged findings and future directions, *Eur. J. Med. Chem.* (2017).
- [9] R. Singla, V. Jaitak, Multitargeted molecular docking study of natural-derived alkaloids on breast cancer pathway components, *Curr. Comput.-Aided Drug Des.* 13 (4) (2017) 294–302.
- [10] Y. Özkay, İ. İşıkdag, Z. Incesu, G. Akalin, Synthesis of 2-substituted-N-[4-(1-methyl-4,5-diphenyl-1H-imidazole-2-yl)phenyl]acetamide derivatives and evaluation of their anticancer activity, *Eur. J. Med. Chem.* 45 (8) (2010) 3320–3328.
- [11] Shaveta, S. Mishra, P. Singh, Hybrid molecules: the privileged scaffolds for various pharmaceuticals, *Eur. J. Med. Chem.* 124 (2016) 500–536.
- [12] M. Decker, Hybrid molecules incorporating natural products: applications in cancer therapy, neurodegenerative disorders and beyond, *Curr. Med. Chem.* 18 (10) (2011) 1464–1475.
- [13] B. Meunier, Hybrid molecules with a dual mode of action: dream or reality?, *Acc. Chem. Res.* 41 (1) (2008) 69–77.
- [14] Y.C. Mayur, G.J. Peters, V.V.S. Rajendra Prasad, C. Lemos, N.K. Sathish, Design of new drug molecules to be used in reversing multidrug resistance in cancer cells, *Curr. Cancer Drug Targets* 9 (3) (2009) 298–306.
- [15] V.R. Solomon, C. Hu, H. Lee, Hybrid pharmacophore design and synthesis of isatin-benzothiazole analogs for their anti-breast cancer activity, *Bioorg. Med. Chem.* 17 (21) (2009) 7585–7592.
- [16] M.P. Fortes, P.B.N. da Silva, T.G. da Silva, T.S. Kaufman, G.C.G. Militão, C.C. Silveira, Synthesis and preliminary evaluation of 3-thiocyanato-1H-indoles as potential anticancer agents, *Eur. J. Med. Chem.* 118 (2016) 21–26.
- [17] J. Zhou, J.-H. Feng, L. Fang, A novel monoterpenoid indole alkaloid with anticancer activity from *Melodinus khasianus*, *Bioorg. Med. Chem. Lett.* 27 (4) (2017) 893–896.
- [18] A. Trawczyński, R. Bujok, Z. Wróbel, K. Wojciechowski, Simple synthesis of pyrrolo[3,2-e]indole-1-carbonitriles, *Beilstein J. Organic Chem.* 9 (2013) 934–941.
- [19] J. Singh Sidhu, R. Singla, Mayank, V. Jaitak, Indole derivatives as anticancer agents for breast cancer therapy: a review, *Anti-Cancer Agents Med. Chem. – Anti-Cancer Agents* 16(2) (2016) 160–173.
- [20] R. Singla, K.B. Gupta, S. Upadhyay, M. Dhiman, V. Jaitak, Design, synthesis and biological evaluation of novel indole-xanthendione hybrids as selective estrogen receptor modulators, *Bioorg. Med. Chem.* 26 (1) (2018) 266–277.
- [21] R. Singla, K.B. Gupta, S. Upadhyay, M. Dhiman, V. Jaitak, Design, synthesis and biological evaluation of novel indole-benzimidazole hybrids targeting estrogen receptor alpha (ER- α), *Eur. J. Med. Chem.* 146 (2018) 206–219.
- [22] T.T.Y. Wang, M.J. Milner, J.A. Milner, Y.S. Kim, Estrogen receptor α as a target for indole-3-carbinol, *J. Nutr. Biochem.* 17 (10) (2006) 659–664.
- [23] J. Singh Sidhu, R. Singla, V. Jaitak, Indole derivatives as anticancer agents for breast cancer therapy: a review, *Anti-Cancer Agents in Medicinal Chemistry (Formerly Current Medicinal Chemistry-Anti-Cancer Agents)* 16(2) (2016) 160–173.
- [24] L.M. Greenberger, T. Annable, K.I. Collins, B.S. Komm, C.R. Lyttle, C.P. Miller, P. G. Satyaswaroop, Y. Zhang, P. Frost, A new antiestrogen, 2-(4-hydroxyphenyl)-3-methyl-1-[4-(2-piperidin-1-yl-ethoxy)-benzyl]-1H-indol-5-ol hydrochloride (ERA-923), inhibits the growth of tamoxifen-sensitive and-resistant tumors and is devoid of uterotrophic effects in mice and rats, *Clin. Cancer Res.* 7 (10) (2001) 3166–3177.
- [25] S.X. Cai, J. Drewe, W. Kemnitzer, Discovery of 4-aryl-4H-chromenes as potent apoptosis inducers using a cell- and caspase-based Anti-cancer Screening Apoptosis Program (ASAP): SAR studies and the identification of novel vascular disrupting agents, *Anticancer Agents Med. Chem.* 9 (4) (2009) 437–456.
- [26] M. Kawase, A. Shah, H. Gaveriya, N. Motohashi, H. Sakagami, A. Varga, J. Molnár, 3,5-Dibenzoyl-1,4-dihydropyridines: synthesis and MDR reversal in tumor cells, *Bioorg. Med. Chem.* 10 (4) (2002) 1051–1055.
- [27] M. Kawase, A. Shah, H. Gaveriya, N. Motohashi, H. Sakagami, A. Varga, J. Molnár, 3,5-dibenzoyl-1,4-dihydropyridines: synthesis and MDR reversal in tumor cells, *Bioorg. Med. Chem.* 10 (4) (2002) 1051–1055.
- [28] X.-F. Zhou, X. Yang, Q. Wang, R.A. Coburn, M.E. Morris, Effects of dihydropyridines and pyridines on multidrug resistance mediated by breast cancer resistance protein: in vitro and in vivo studies, *Drug Metab. Dispos.* 33 (8) (2005) 1220.
- [29] J. Ghosh, P. Biswas, T. Sarkar, M.G.B. Drew, C. Bandyopadhyay, A one-pot three-component reaction in aqueous micellar medium: an easy route to chromeno [2,3-b]quinolinone, *Tetrahedron Lett.* 55 (18) (2014) 2924–2928.
- [30] S.A. Moallem, N. Dehghani, S. Mehri, S. Shahsavand, M. Alibolandi, F. Hadizadeh, Synthesis of novel 1,8-acridinediones derivatives: Investigation of MDR reversibility on breast cancer cell lines T47D and tamoxifen-resistant T47D, *Res. Pharm. Sci.* 10 (3) (2015) 214–221.
- [31] A. Jamalian, A. Shafiee, B. Hemmateenejad, M. Khoshneviszadeh, R. Miri, A. Madadkar-Sobhani, S.Z. Bathaie, A.A. Moosavi-Movahedi, Novel imidazole derivatives of 1,8-acridinedione as potential DNA-intercalating agents, *J. Iran. Chem. Soc.* 8 (4) (2011) 1098–1112.

- [32] A. Kumar, S. Sharma, R.A. Maurya, J. Sarkar, Diversity oriented synthesis of benzoxanthene and benzochromene libraries via one-pot, three-component reactions and their anti-proliferative activity, *J. Combinatorial Chem.* 12 (1) (2009) 20–24.
- [33] F. Al-Omran, R.M. Mohareb, A.A. El-Khair, New route for synthesis, spectroscopy, and X-ray studies of 2-[aryl-(6'-hydroxy-4', 4'-dimethyl-2'-oxocyclohex-6'-enyl) methyl]-3-hydroxy-5, 5-dimethylcyclohex-2-enone and 1, 8-dioxo-octahydroxanthenes and antitumor evaluation, *Med. Chem. Res.* 23 (4) (2014) 1623–1633.
- [34] N.M. Sabry, H.M. Mohamed, E.S.A.E.H. Khattab, S.S. Motlaq, A.M. El-Agrody, Synthesis of 4H-chromene, coumarin, 12H-chromeno[2,3-d]pyrimidine derivatives and some of their antimicrobial and cytotoxicity activities, *Eur. J. Med. Chem.* 46 (2) (2011) 765–772.
- [35] G. Li, S. Thomas, J.J. Johnson, Polyphenols from the mangosteen (*Garcinia mangostana*) fruit for breast and prostate cancer, *Front. Pharmacol.* 4 (2013) 80.
- [36] Y.-S. Won, J.-H. Lee, S.-J. Kwon, J.-Y. Kim, K.-H. Park, M.-K. Lee, K.-I. Seo, α -Mangostin-induced apoptosis is mediated by estrogen receptor α in human breast cancer cells, *Food Chem. Toxicol.* 66 (2014) 158–165.
- [37] S. Hayes, Remington: the science and practice of pharmacy, volume I and volume II. Twenty-second edition, *J. Med. Library Assoc.: JMLA* 102 (3) (2014) 220–221.
- [38] T.J. Hou, W. Zhang, K. Xia, X.B. Qiao, X.J. Xu, ADME evaluation in drug discovery. 5. Correlation of Caco-2 permeation with simple molecular properties, *J. Chem. Inf. Comput. Sci.* 44 (5) (2004) 1585–1600.
- [39] S. Leon, B. Andrew, *Applied Biopharmaceutics & Pharmacokinetics*, McGraw-Hill, New York, 2005.
- [40] E. Raschi, L. Ceccarini, F. De Ponti, M. Recanatini, hERG-related drug toxicity and models for predicting hERG liability and QT prolongation, *Expert Opin. Drug Metab. Toxicol.* 5 (9) (2009) 1005–1021.
- [41] F. Ntie-Kang, L.L. Lifongo, J.A. Mbah, L.C.O. Owono, E. Megnassan, L.M.A. Mbaze, P.N. Judson, W. Sippl, S.M. Efang, In silico drug metabolism and pharmacokinetic profiles of natural products from medicinal plants in the Congo basin, *In silico pharmacology* 1(1) (2013) 12.
- [42] H.M. Weir, R.H. Bradbury, M. Lawson, A.A. Rabow, D. Buttar, R.J. Callis, J.O. Curwen, C. de Almeida, P. Ballard, M. Hulse, AZD9496: an oral estrogen receptor inhibitor that blocks the growth of ER-positive and ESR1-mutant breast tumors in preclinical models, *Cancer Res.* (2016).
- [43] P. Ertl, A. Schuffenhauer, Estimation of synthetic accessibility score of drug-like molecules based on molecular complexity and fragment contributions, *J. Cheminformatics* 1 (1) (2009) 8.
- [44] H.G. Kathrotiya, M.P. Patel, Microwave-assisted synthesis of 3'-indolyl substituted 4H-chromenes catalyzed by DMAP and their antimicrobial activity, *Med. Chem. Res.* 21 (11) (2012) 3406–3416.
- [45] S.Y. Park, Y.M. Lee, K. Kwac, Y. Jung, O.H. Kwon, Alcohol Dimer is Requisite to Form an Alkyl Oxonium Ion in the Proton Transfer of a Strong (Photo)Acid to Alcohol, *Chemistry (Weinheim an der Bergstrasse, Germany)* 22(13) (2016) 4340–4344.
- [46] I. Sehout, R. Boulcina, B. Boumoud, T. Boumoud, A. Debache, Solvent-free synthesis of polyhydroquinoline and 1, 8-dioxodecahydroacridine derivatives through the Hantzsch reaction catalyzed by a natural organic acid: a green method, *Synth. Commun.* 47 (12) (2017) 1185–1191.
- [47] M. Al-Bader, C. Ford, B. Al-Ayadhy, I. Francis, Analysis of estrogen receptor isoforms and variants in breast cancer cell lines, *Exp. Therapeutic Med.* 2 (3) (2011) 537–544.
- [48] A. Strom, J. Hartman, J.S. Foster, S. Kietz, J. Wimalasena, J.A. Gustafsson, Estrogen receptor beta inhibits 17 β -estradiol-stimulated proliferation of the breast cancer cell line T47D, *PNAS* 101 (6) (2004) 1566–1571.
- [49] Z. Li, M. Yan, Z. Li, M. Vuki, D. Wu, F. Liu, W. Zhong, L. Zhang, D. Xu, A multiplexed screening method for agonists and antagonists of the estrogen receptor protein, *Anal. Bioanal. Chem.* 403 (5) (2012) 1373–1384.
- [50] D.A. Peterson, Confocal Microscopy, *Encyclopedia of Movement Disorders*, Academic Press, Oxford, 2010, pp. 250–252.
- [51] J. Kurebayashi, T. Otsuki, H. Kunisue, K. Tanaka, S. Yamamoto, H. Sonoo, Expression levels of estrogen receptor- α , estrogen receptor- β , coactivators, and corepressors in breast cancer, *Clin. Cancer Res.* 6 (2) (2000) 512–518.
- [52] C.K. Osborne, R. Schiff, Mechanisms of endocrine resistance in breast cancer, *Annu. Rev. Med.* 62 (2011) 233–247.
- [53] P. La Rosa, M. Pellegrini, P. Totta, F. Acconcia, M. Marino, Xenoestrogens alter estrogen receptor (ER) α intracellular levels, *PLOS ONE* 9 (2) (2014) e88961.
- [54] M. Dhiman, M.P. Zago, S. Nunez, A. Amoroso, H. Rementeria, P. Dousset, F.N. Burgos, N.J. Garg, Cardiac-oxidized antigens are targets of immune recognition by antibodies and potential molecular determinants in chagas disease pathogenesis, *PLOS ONE* 7 (1) (2012) e28449.
- [55] A.K. Mantha, M. Dhiman, G. Tagliatalata, R.J. Perez-Polo, S. Mitra, Proteomic study of amyloid beta (25–35) peptide exposure to neuronal cells: impact on APE1/Ref-1's protein–protein interaction, *J. Neurosci. Res.* 90 (6) (2012) 1230–1239.
- [56] N.J. Kruger, The Bradford method for protein quantitation, in: J.M. Walker (Ed.), *The Protein Protocols Handbook*, Humana Press, Totowa, NJ, 2009, pp. 17–24.